A Constrained Instrumental Variable Method for Identification of Industrial Robots

Fabio Ardiani, Alexandre Janot, Mourad Benoussaad

A Constrained Instrumental Variable Method for Identification of Industrial Robots

Fabio Ardiani[1], Alexandre Janot[2] and Mourad Benoussaad[3]

***Abstract*— Robot identification is a prolific topic with a long history of results spanning decades. In recent years, there has been a renewal of interest in this problem mainly due to a rapid increase in robotic hardware platforms capable of accurate model-based control. The standard approach exploits the inverse dynamic model's linearity to dynamic parameters and uses the linear least-squares (LS) estimation. Since we identify robots with closed-loop procedures, a correlation between errors remains, and we should prefer the Instrumental Variable (IV) method over the LS estimation. Thanks to the increase in computational power, recent works suggest inserting physical constraints to ensure the physical plausibility of estimates. These works have emphasized the usefulness of these physical constraints, but few papers consider their insertion into IV methods, the consistency and optimality of estimates, and the effect of constraints on estimates not addressed. This paper presents a new constrained IV approach that uses physical constraints. It consists of two nested iterative algorithms: an outer one that is a standard IV method and an inner one that accounts for the constraints solved by a Gauss-Newton algorithm. Besides, the conditions to obtain consistent and optimal estimates are emphasized. Experimental results and comparisons with other methods carried out with the TX40 robot show the feasibility and effectiveness of such an IV method: we can identify 60 physically consistent parameters in less than one minute.**

I. Introduction

A. Topic and general context

Robot identification involves identifying the dynamic parameters (mass, center of mass, rotational inertia, and friction) that influence the relationship between applied forces and resultant accelerations. It is a classical problem, with results spanning recent decades; see the survey in [1]. Recent years have witnessed a renewal in this problem due in part to a rapid increase in robotic hardware platforms capable of accurate model-based control [2]–[4], growth in the utilization of force-controlled actuators, [5], [6], and better control techniques [7], [8] and mechanical design [9].

The conventional method, referred to as the Inverse Dynamic Identification Model with Least-Squares estimation (IDIM-LS method), [10], exploits the linearity of the inverse dynamic model (IDM) to the dynamic parameters. However, since we identify robots with closed-loop procedures, it induces a correlation between errors that may lead to inconsistent IDIM-LS estimates, even in the case of proper data filtering, [11], [12].

[1]The author is with Nimble One, Toulouse, France fabio.ardiani@nimbleone.io

[2]The author is with the DTIS, ONERA, Paris Saclay University, Palaiseau, France alexandre.janot@onera.fr

[2]The author is with the LGP-UTTOP, University of Toulouse, Tarbes, France mourad.benoussaad@uttop.fr

Consequently, instrumental variable (IV) techniques or Output-Error (OE) methods allow the users to get consistent estimates despite the correlation between errors, [13]. In [10] and [12], the authors have developed an OE approach named the Direct and Inverse Dynamics Identification Models approach (DIDIM) and an IV approach called IDIM-IV, respectively. Both methods combine the direct and inverse dynamic models and converge quickly. However, because of modeling errors, like other unconstrained approaches, DIDIM and IDIM-IV could not guarantee that the direct dynamic model (DDM) would be well-posed during their iterations. Using physical constraints can address this deficiency for unconstrained identification approaches.

B. Constrained identification methods for robots and in Econometrics

In [14], the authors have proposed an approach to insert physical constraints. In contrast, [15] has further improved it by noting that the set of all possible inertial parameters, which ensures a positive definite mass matrix, is known to be convex. The authors suggest using 4x4 linear matrix inequalities (LMIs) posed over the 10 inertial parameters of each rigid body. This constrained method combining IDIM-LS and physical constraints is called the Physically-Consistent IDIM-LS method (PC-IDIM-LS). It was successfully applied in [15]–[18]. However, these works did not treat the statistical properties of PC-IDIM-LS. Consequently, [19] provides a complete statistical analysis of PC-IDIM-LS and suggests inserting the physical constraints into the DIDIM method. This constrained OE method, PC-DIDIM, has been validated on a 6 degrees-of-freedom (DOF) robot and provides physically and statistically consistent estimates. Besides, the results showed that PC-DIDIM is more robust against modeling errors than other unconstrained OE approaches.

In Econometrics, constrained identification has a long history; see, e.g., [20]–[27], and the references therein. Accounting for the equality and/or inequality constraints explicitly is necessary to develop some identification methods and hypothesis testing. Unsurprisingly, procedures with inequality constraints are the most complex, [22] and [25], chapter 21. To understand how constraints affect estimates, it is not rare that the authors introduce intuitive explanations and/or examples, and they often relate the constrained and unconstrained estimates. Indeed, provided that the unconstrained estimates are consistent and satisfy the constraints, they must stick to the constrained estimates. Finally, these works consider the identifiable parameters only.

C. Motivations and contributions of the paper

The papers mentioned above in Robotics have not considered IV approaches while they have the reputation of being more robust against modeling errors than OE methods, [28]. It could be wise to insert physical constraints into IDIM-IV to ensure the physical feasibility of IV estimates while securing the consistency of estimates. This way, we could get a constrained IV approach that is more robust than constrained OE methods. Besides, the authors used the standard dynamic parameters that are not all identifiable, [29], [30]. It is somehow puzzling to deal with parameters that do not affect the dynamics. Indeed, we can hardly see how constraints could make them identifiable or how constraints on such parameters could impact dynamics. This point is not discussed in these papers, whereas parameters' identifiability is a key concept in System identification, see [11], [13], [31] among others. Finally, they did not explain why the constraints are not overly restrictive while it is known that the choice of constraints impacts the optimization process, [32], [25] chapter 21.

Inserting constraints implies the calculation of Lagrangian multipliers and slack variables, see [25], [32], [33], and these variables produce a nonlinear problem that is solved with Newton's method. So, from a problem that is initially linear to the dynamic parameters, we finally deal with a nonlinear problem because of the Lagrangian multipliers and slack variables. The way to solve the constrained problem is not tackled in the abovementioned papers.

It comes out that dealing with constrained identification methods is challenging because we must: choose constraints that are not overly restrictive, choose a criterion that is suitable and easy to interpret for users, analyze the impact of constraints on estimates, and deal with nonlinear optimization. This outcome may explain why constrained identification methods are not as popular as the unconstrained procedures although they are of great importance, see, e.g., [21], [22], [26]. It may also explain why a consistency analysis, or at least a discussion on conditions that allow us to get consistent estimates, is missing in [7], [14], [15], [17].

The first contribution of this paper proposes a constrained IV approach, called PC-IDIM-IV, by expanding [34]. We analyze the consistency and efficiency of PC-IDIM-IV estimates and the effect of constraints, and we show how to detect overly constrained.

The second contribution concerns the experimental validations. We validate and compare PC-IDIM-IV to other standard approaches employed in robotics on the TX40 robot. The experimental results show we can identify 60 dynamic parameters with PC-IDIM-IV in less than one minute.

D. Organization of the paper

Section II reviews the background of robotic modeling and identification, while Section III describes the PC-IDIM-IV method and gives the conditions to get consistent estimates. Details on the experimental setup of the TX40 robot and the experimental results are shown in Section IV. Finally, Section V concludes this paper.

II. Background

A. Equations of motion of rigid robot model

The Inverse Dynamic Model (IDM) of a n-DOF rigid robot expresses the joint torques as a function of the joint positions, velocities, and accelerations, [29], [35]. It is given by

$$\boldsymbol{\tau} = \mathbf{M}(\mathbf{q})\ddot{\mathbf{q}} + \mathbf{N}(\mathbf{q}, \dot{\mathbf{q}}) + \boldsymbol{\tau_f}, \tag{1}$$

where $\boldsymbol{\tau} \in \mathbb{R}^n$ is the vector of the joint torques; $\mathbf{q}, \dot{\mathbf{q}}, \ddot{\mathbf{q}} \in \mathbb{R}^n$ are the vectors of joint positions, velocities and accelerations, respectively; $\mathbf{N}(\mathbf{q}, \dot{\mathbf{q}}) \in \mathbb{R}^n$ is the vector of Coriolis, centrifugal and gravitational torques; $\mathbf{M}(\mathbf{q}) \in \mathbb{R}^{(n\times n)}$ is the symmetric and positive definite inertia matrix; and $\boldsymbol{\tau_f} \in \mathbb{R}^n$ are friction torques. Usually, we choose, see [36],

$$\tau_{f_j} = F_{c_j}\text{sign}(\dot{q}_j) + F_{v_j}\dot{q}_j\,, \tag{2}$$

where τ_{f_j} is the joint j friction vector; F_{c_j} and F_{v_j} are Coulomb and viscous friction parameters, respectively. The dynamics of link j includes 11 standard inertial parameters: XX_j, XY_j, XZ_j, YY_j, YZ_j and ZZ_j are the components of the inertia tensor, $\mathbf{I}_j$, considered from the origin of the link; MX_j, MY_j and MZ_j are the components of its first moment of inertia, with $\mathbf{MS}_j = [MX_j, MY_j, MZ_j]^T$; m_j is its mass; I_{a_j} is the actuator's inertia. F_{c_j} and F_{v_j} complete the set, and the dynamics of a link j is defined by 13 standard parameters. Because the kinetic and potential energies are linear to the standard parameters, so is the IDM, [29], [35]. We can write equation (1) as

$$\boldsymbol{\tau} = \mathbf{IDM}_f(\mathbf{q}, \dot{\mathbf{q}}, \ddot{\mathbf{q}})\boldsymbol{\beta}_f, \tag{3}$$

where $\mathbf{IDM}_f(\mathbf{q}, \dot{\mathbf{q}}, \ddot{\mathbf{q}}) \in \mathbb{R}^{(n\times n_c)}$ is the matrix of the IDM concerning the vector $\boldsymbol{\beta}_f \in \mathbb{R}^{n_c}$ of the n_c standard parameters, with $n_c = 13 \cdot n$. However, all the standard parameters are not identifiable because some are regrouped via linear relations while others have no contribution. We can identify a set of so-called base parameters determined by the expressions of kinetic and potential energies, [30]. The IDM (3) reduces to

$$\boldsymbol{\tau} = \mathbf{IDM}(\mathbf{q}, \dot{\mathbf{q}}, \ddot{\mathbf{q}})\boldsymbol{\beta}, \tag{4}$$

where $\mathbf{IDM}(\mathbf{q}, \dot{\mathbf{q}}, \ddot{\mathbf{q}}) \in \mathbb{R}^{(n\times n_b)}$ is the matrix of the IDM to the vector $\boldsymbol{\beta} \in \mathbb{R}^{n_b}$ of the n_b base parameters. The joint j torque, τ_j, is given by

$$\tau_j = \mathbf{IDM}_j(\mathbf{q}, \dot{\mathbf{q}}, \ddot{\mathbf{q}})\boldsymbol{\beta}_j, \tag{5}$$

where $\mathbf{IDM}_j(\mathbf{q}, \dot{\mathbf{q}}, \ddot{\mathbf{q}}) \in \mathbb{R}^{(n\times n_{b_j})}$ is the matrix of the joint j IDM to the vector $\boldsymbol{\beta}_j \in \mathbb{R}^{n_{b_j}}$ of the n_{b_j} base parameters of the link j; and $n_b = \sum n_{b_j}$.

B. Data acquisition and controls

For safety considerations, robots are identified under closed-loop control using linear controllers (e.g., PD, PID, etc., see [29]). The torque delivered by each motor τ_j is then given by

$$\tau_j = C_j(s)(q_{r_j} - q_{m_j})\,, \tag{6}$$

where $C_j(s)$ is the transfer function of the joint j controller; q_{r_j} the reference; q_{m_j} the measured angle of the joint position; and s is the Laplace variable. $C_j(s)$ is normally a PD or PID in

practice, see [29]. The bandwidth of the position closed-loop, denoted as ω_{dyn}, is usually less than 10Hz.

From this process, the data available for identification includes the measured angles $\mathbf{q}_m \in \mathbb{R}^n$, their references $\mathbf{q}_r$, and the input torques $\boldsymbol{\tau}$.

C. Data filtering and construction of the Inverse Dynamic Identification Model

The IDM given in (4) is sampled n_s times while the robot tracks reference trajectories. In (4), $\mathbf{q}$ is estimated with $\hat{\mathbf{q}}$ obtained through the filtering of $\mathbf{q}_m$ with a lowpass Butterworth filter in both the forward and reverse directions. One chooses ω_{bf}, the cutoff frequency of the Butterworth filter, as $\omega_{bf} = 5.0 \cdot \omega_{dyn}$, [10]. Then, we calculate $\hat{\dot{\mathbf{q}}}, \hat{\ddot{\mathbf{q}}}$ with a central differentiation algorithm of $\hat{\mathbf{q}}$, [10]. We get this over-determined linear system

$$\mathbf{y}_m = \mathbf{X}_m(\hat{\mathbf{q}}, \hat{\dot{\mathbf{q}}}, \hat{\ddot{\mathbf{q}}})\boldsymbol{\beta} + \boldsymbol{\varepsilon}_m \,, \tag{7}$$

where $\mathbf{y}_m \in \mathbb{R}^{r_s}$ is the vector of measured torques with $r_s = n_s \times n$; $\mathbf{X}_m(\hat{\mathbf{q}}, \hat{\dot{\mathbf{q}}}, \hat{\ddot{\mathbf{q}}}) \in \mathbb{R}^{(r_s \times n_b)}$ is the observation matrix built from the sampling of $\mathbf{IDM}(\hat{\mathbf{q}}, \hat{\dot{\mathbf{q}}}, \hat{\ddot{\mathbf{q}}})$; and $\boldsymbol{\varepsilon}_m \in \mathbb{R}^{r_s}$ is the vector of error terms.

In practice, the torque is perturbed by high-frequency ripples removed before the identification with a parallel lowpass filtering of each column of $\mathbf{X}_m$ and the vector $\mathbf{y}_m$. This parallel low-pass filtering is part of a decimation procedure, i.e., resampling to keep one sample over n_d. We choose ω_{df}, the cutoff frequency of the decimation filter, as $\omega_{df} = 2.0 \cdot \omega_{dyn}$, [10]. One has $n_d = \omega_{samp}/\omega_{dyn}$, where ω_{samp} is the sampling frequency. We finally obtain the following *filtered* over-determined linear system to $\boldsymbol{\beta}$ called the Inverse Dynamic Identification Model (IDIM):

$$\mathbf{y} = \mathbf{X}(\hat{\mathbf{q}}, \hat{\dot{\mathbf{q}}}, \hat{\ddot{\mathbf{q}}})\boldsymbol{\beta} + \boldsymbol{\varepsilon} \,, \tag{8}$$

where $\mathbf{y} \in \mathbb{R}^r$ is the vector of filterred torques with $r = n_e \times n$; $\mathbf{X}(\hat{\mathbf{q}}, \hat{\dot{\mathbf{q}}}, \hat{\ddot{\mathbf{q}}}) \in \mathbb{R}^{(r \times n_b)}$ is the filtered observation matrix; and $\boldsymbol{\varepsilon} \in \mathbb{R}^r$ is the vector of the filtered error.

We assume that $\boldsymbol{\varepsilon}$ has the following covariance matrix, $\boldsymbol{\Omega} = \text{diag}\left(\sigma_1^2\mathbf{I}_{n_e}, \ldots, \sigma_n^2\mathbf{I}_{n_e}\right)$, where $\mathbf{I}_{n_e}$ is the $n_e \times n_e$ identity matrix. The errors are assumed serially uncorrelated and with finite variance. In the appendix VI-A, we give details about data filtering and how it is linked with the process commonly applied in the Automatic Control community.

D. The IDIM-LS method

The LS estimates of (8) and their covariance matrix are given by

$$\begin{aligned} \hat{\boldsymbol{\beta}}_{LS} &= \left(\mathbf{X}^T\mathbf{X}\right)^{-1}\mathbf{X}^T\mathbf{y} \\ \hat{\boldsymbol{\Sigma}}_{LS} &= \left(\mathbf{X}^T\boldsymbol{\Omega}^{-1}\mathbf{X}\right)^{-1} , \end{aligned} \tag{9}$$

see, e.g., [37]. Following the procedure in [10], each σ_j is estimated from the standard deviation of the error in an IV fit to the joint j torque, τ_j, alone. This method combines IDIM and LS estimation and is termed the IDIM-LS method. The IDIM-LS estimates are theoretically biased because robots are identified with closed-loop procedures that induce noise correlation [11], [12]. To overcome this issue, IV we can employ IV procedures.

E. The IDIM-IV method

IV method has a long history in Econometrics, [37], chapter 7, [38] chapter 8, [39], [40], chapter 15, and [24], chapter 9, among others, and in Automatic Control [11], [13], [28], [41], [42], among others.

IV methods are usually iterative procedures that deal with noise correlation by employing an instrumental matrix denoted $\mathbf{Z} \in \mathbb{R}^{(r \times n_b)}$, [11], [28]. $\mathbf{Z}$ must fulfill two properties to secure consistency: $\mathbf{Z}$ must be correlated with $\mathbf{X}$ so that $\mathbf{Z}^T\mathbf{X}$ is invertible, and must be uncorrelated with the noise $\boldsymbol{\varepsilon}$, see [11]. Formally, we have

$$\begin{aligned} rank\left(\mathbf{Z}^T\mathbf{X}\right) &= n_b \\ E\left(\mathbf{Z}^T\boldsymbol{\varepsilon}\right) &= \mathbf{0} \,, \end{aligned} \tag{10}$$

where $E()$ is the expectation operator.

According to [11], we can construct such a matrix $\mathbf{Z}$ by simulating an *auxiliary* model based on previous IV estimates, denoted as $\hat{\boldsymbol{\beta}}_{IV}^{(k-1)}$. For robot identification, this auxiliary model is the DDM given by

$$\ddot{\mathbf{q}} = \mathbf{M}(\mathbf{q})^{-1}\left(\boldsymbol{\tau} - \mathbf{N}(\mathbf{q}, \dot{\mathbf{q}}) - \boldsymbol{\tau}_{\boldsymbol{f}}\right) , \tag{11}$$

that is simulated using $\hat{\boldsymbol{\beta}}_{IV}^{(k-1)}$ and considering the same reference trajectory and control law for the actual and simulated robot [12]. Hence, at iteration *k*, the IV estimates and their covariance matrix are given by

$$\begin{aligned} \hat{\boldsymbol{\beta}}_{IV}^{(k)} &= (\mathbf{Z}^T\mathbf{X})^{-1}\mathbf{Z}^T\mathbf{y} \\ \hat{\boldsymbol{\Sigma}}_{IV} &= \left(\mathbf{Z}^T\boldsymbol{\Omega}^{-1}\mathbf{Z}\right)^{-1} , \end{aligned} \tag{12}$$

where $\mathbf{Z} = \mathbf{X}(\mathbf{q}_S, \dot{\mathbf{q}}_S, \ddot{\mathbf{q}}_S, \hat{\boldsymbol{\beta}}_{IV}^{(k-1)}$ results from the sampling and decimation of $\mathbf{IDM}\left(\mathbf{q}_S, \dot{\mathbf{q}}_S, \ddot{\mathbf{q}}_S\right)$, where $(\mathbf{q}_S, \dot{\mathbf{q}}_S, \ddot{\mathbf{q}}_S)$ are the simulated joint positions, velocities and accelerations, respectively. Note that we use $\mathbf{Z}$ instead of $\mathbf{Z}^{(k)}$ for better clarity. Each σ_j is estimated from the standard deviation of the error in an IV fit to the joint j torque, τ_j, alone. This method combines IDIM and IV estimation and is termed the IDIM-IV method.

Let $\mathbf{X}_{nf} \in \mathbb{R}^{(r \times n_b)}$ be the noise-free observation matrix with $\mathbf{X} = \mathbf{X}_{nf} + \mathbf{V}$; $\mathbf{V} \in \mathbb{R}^{(r \times n_b)}$ being the matrix gathering all the noise within $\mathbf{X}$ with $E(\mathbf{V}) = \mathbf{0}$. In [11], chapter 6, the author showed that $\mathbf{Z}$ is an approximation of $\mathbf{X}_{nf}$, i.e., $\mathbf{Z} \approx \mathbf{X}_{nf}$, provided there are no modeling errors or such errors prove to be negligible compared to noises. In [11], chapter 6, the author showed that one has

$$\hat{\boldsymbol{\Sigma}}_{IV} \succeq \boldsymbol{\Sigma}_{IV}^{opt} \,, \tag{13}$$

where

$$\boldsymbol{\Sigma}_{IV}^{opt} = \left(\mathbf{X}_{nf}^T\boldsymbol{\Omega}^{-1}\mathbf{X}_{nf}\right)^{-1} \tag{14}$$

is the lower bound, [11], [13], [38]. If $\hat{\boldsymbol{\Sigma}}_{IV} \approx \boldsymbol{\Sigma}_{IV}^{opt}$, then we reach the *optimal* covariance matrix of the IV estimates. Consequently, $\mathbf{X}_{nf}$ is the *optimal* instrumental matrix. This result is consistent with [13].

F. DIDIM method

Now, we describe briefly the Direct and Inverse Dynamic Identification Models (DIDIM) method; all the details are given in [43]. DIDIM is a closed-loop input-error approach that minimizes the following criterion

$$||\mathbf{y} - \mathbf{y}_s(\boldsymbol{\beta})||_2^2, \tag{15}$$

where $\mathbf{y}_s(\boldsymbol{\beta}) \in \mathbb{R}^r$ is the sampled vector of simulated torques. To identify the parameters, we run an iterative algorithm as usually done with output- or input-error methods, see [43].

Because of the control (6), $\frac{\partial \mathbf{q}_s}{\partial \boldsymbol{\beta}} \approx \mathbf{0}$, $\frac{\partial \dot{\mathbf{q}}_s}{\partial \boldsymbol{\beta}} \approx \mathbf{0}$, and $\frac{\partial \ddot{\mathbf{q}}_s}{\partial \boldsymbol{\beta}} \approx \mathbf{0}$ hold. Hence at iteration k, we can show that the DIDIM estimates and their covariance matrix are given by

$$\begin{aligned} \hat{\boldsymbol{\beta}}_{DIDIM}^{(k)} &= (\mathbf{Z}^T\mathbf{Z})^{-1}\mathbf{Z}^T\mathbf{y} \\ \hat{\boldsymbol{\Sigma}}_{DIDIM} &= \left(\mathbf{Z}^T\boldsymbol{\Omega}^{-1}\mathbf{Z}\right)^{-1}, \end{aligned} \tag{16}$$

and this process is iterated until convergence. Note that we have $\mathbf{Z} = \mathbf{X}(\mathbf{q}_S, \dot{\mathbf{q}}_S, \ddot{\mathbf{q}}_S, \hat{\boldsymbol{\beta}}_{DIDIM}^{(k-1)})$ in this case.

G. Physical constraints

In [15], the authors have provided linear matrix inequality (LMI) constraints that are necessary and sufficient for the physical plausibility of $\boldsymbol{\beta}_{f_j}$. These results hinge on the so-called pseudo-inertia matrix $\mathbf{J}(\boldsymbol{\beta}_{f_j}) \in \mathbb{R}^{(4\times4)}$ of a rigid body defined by

$$\mathbf{J}(\boldsymbol{\beta}_{f_j}) = \begin{bmatrix} \frac{1}{2}\mathrm{tr}(\mathbf{I}_j)\mathbf{I}_3 - \mathbf{I}_j & \mathbf{M}\mathbf{S}_j \\ \mathbf{M}\mathbf{S}_j^T & m_j \end{bmatrix}, \tag{17}$$

where $\mathbf{I}_3$ is the (3×3) identity matrix. Then, the parameters $\boldsymbol{\beta}_{f_j}$ are physically consistent if and only if

$$\mathbf{J}(\boldsymbol{\beta}_{f_j}) \succ \mathbf{0}. \tag{18}$$

Since we further impose $I_{a_j} > 0, F_{v_j} > 0, F_{c_j} > 0$ for $j = 1, \cdots, n$, the physical constraints are finally

$$\mathbf{J}(\boldsymbol{\beta}_{f_j}) \succ \mathbf{0}, I_{a_j} > 0, F_{v_j} > 0, F_{c_j} > 0. \tag{19}$$

This development allows a Physically-Consistent IDIM-LS problem (PC-IDIM-LS) to be formulated as a semi-definite program (SDP). Besides, in [19], the authors showed that the constraints (19) turn to inequality constraints so that we obtain the following constrained problem

$$\begin{aligned} &\text{minimize} \quad f_0(\boldsymbol{\beta}_f), \\ &\text{subject to} \quad h_i(\boldsymbol{\beta}_f) \geq 0, \text{ for } i = 1, \cdots, p, \end{aligned} \tag{20}$$

where $f_0(\boldsymbol{\beta}_f) = ||\boldsymbol{\varepsilon}||_2^2 = ||\mathbf{y} - \mathbf{X}_f\boldsymbol{\beta}_f||_2^2$; $\mathbf{X}_f \in \mathbb{R}^{(r\times n_c)}$ results from the sampling of $\mathbf{IDM}_f\left(\hat{\mathbf{q}}, \hat{\dot{\mathbf{q}}}, \hat{\ddot{\mathbf{q}}}\right)$; $h_i(\boldsymbol{\beta}_f)$ are the constraints obtained from (19); and $p = 7 \cdot n$ is the number of constraints.

In [19], the authors analyze PC-IDIM-LS. They proved that the PC-IDIM-LS estimates are both physically and statistically consistent if $\mathrm{plim}_{r\to\infty}\left(\frac{1}{r}\mathbf{X}_f^T\boldsymbol{\varepsilon}\right) = \lim_{r\to\infty}\left(\frac{1}{r}E\left(\mathbf{X}_f^T\boldsymbol{\varepsilon}\right)\right) = \mathbf{0}$, so if $E\left(\mathbf{X}_f^T\boldsymbol{\varepsilon}\right) = \mathbf{0}$, where plim is the limit in probability as r tends to ∞. However, the authors have not analyzed the impact of the constraints since they considered them fulfilled. Besides, it is somehow puzzling to use standard parameters, whereas we know we can identify only the base parameters. This point is not treated in [14], [17], [19], [44].

III. Physically Consistent IDIM-IV

A. The Two Stage Least-Squares approach

The Two Stage Least-Squares (2SLS) approach considers the following system instead of (8), see [37], [40], [45], [46],

$$\begin{aligned} \mathbf{y} &= \mathbf{X}\boldsymbol{\beta} + \boldsymbol{\varepsilon} \\ \mathbf{X} &= \mathbf{Z}\boldsymbol{\Pi} + \mathbf{V}, \end{aligned} \tag{21}$$

where $\mathbf{Z} \in \mathbb{R}^{(r\times n_z)}$ is an instrumental matrix with $n_z \geq n_b$; $\boldsymbol{\Pi} \in \mathbb{R}^{(n_z\times n_b)}$ is a matrix of coefficients that evaluates the correlation between $\mathbf{Z}$ and $\mathbf{X}$. In Econometrics, researchers employ more instruments than regressors, i.e., columns of $\mathbf{X}$, because the models are mostly empirical. Note that one has $rank(\boldsymbol{\Pi}) = n_b$ if $\mathbf{Z}$ and $\mathbf{X}$ are well correlated, see [37], [40], [45], [46].

The 2SLS method is executed as follows. In the first stage, we calculate the LS estimate of $\boldsymbol{\Pi}$ given by

$$\hat{\boldsymbol{\Pi}} = \left(\mathbf{Z}^T\mathbf{Z}\right)^{-1}\mathbf{Z}^T\mathbf{X}. \tag{22}$$

If $rank\left(\hat{\boldsymbol{\Pi}}\right) = n_b$, then $\mathbf{Z}$ and $\mathbf{X}$ are well correlated, and we can run the second stage; otherwise, they are not, meaning that $\mathbf{Z}^T\mathbf{X}$ is not invertible, and we cannot pursue further. In the second stage, $\mathbf{X}$ is replaced by $\hat{\mathbf{X}} = \mathbf{Z}\hat{\boldsymbol{\Pi}}$, and we compute the 2SLS estimates of $\boldsymbol{\beta}$ and their covariance matrix given by

$$\begin{aligned} \hat{\boldsymbol{\beta}}_{2SLS} &= \left(\hat{\mathbf{X}}^T\mathbf{X}\right)^{-1}\hat{\mathbf{X}}^T\mathbf{y} \\ \hat{\boldsymbol{\Sigma}}_{SLS} &= \left(\hat{\mathbf{X}}^T\boldsymbol{\Omega}^{-1}\hat{\mathbf{X}}\right)^{-1}. \end{aligned} \tag{23}$$

Note that if $n_z = n_b$, the 2SLS estimates reduce to the classical IV estimates (12), see [37] chapter 7 and appendix VI-C. Note further that one has

$$\hat{\mathbf{X}} = \mathbf{P}_{\mathbf{Z}}\mathbf{X}, \tag{24}$$

where $\mathbf{P}_{\mathbf{Z}} = \mathbf{Z}(\mathbf{Z}^T\mathbf{Z})^{-1}\mathbf{Z}^T$, with $\mathbf{P}_{\mathbf{Z}} \in \mathbb{R}^{(r\times r)}$, is the orthogonal projector onto the space generated by the columns of $\mathbf{Z}$. Interestingly, in Econometrics researchers and specialists make no difference between IV and 2SLS, also known as the Generalized IV method, and generally use (23). Interested readers can find a complete theoretical description of the 2SLS with various econometric applications in [24], [37], [38], [40], [45], [46], and the references therein.

From now on, we assume that $n_z = n_b$, as is usually the case in robotics. We further note that $\hat{\boldsymbol{\Pi}}$ is a consistent estimate of $\boldsymbol{\Pi}$, i.e., $\mathrm{plim}_{r\to\infty}\hat{\boldsymbol{\Pi}} = \boldsymbol{\Pi}$. In the rest of the analysis, we assume that

$$rank\left(\hat{\boldsymbol{\Pi}}\right) = n_b, \tag{25}$$

holds, and this implies implies $rank(\boldsymbol{\Pi}) = n_b$, see appendix VI-B. Finally, we indifferently use the term IV or 2SLS as done in Econometrics.

B. Choice of physical constraints and criterion

Because the constraints given by (19) use the standard parameters that are, as recalled in Section II, redundant in the IDM, we propose physical constraints on the base parameters only. This choice makes sense since the base parameters are

linear combinations of the standard parameters, [30]. Indeed, we have

$$\boldsymbol{\beta} = \boldsymbol{\beta}_I + \mathbf{K}\boldsymbol{\beta}_{NI}\,, \tag{26}$$

where $\boldsymbol{\beta}_I \in \mathbb{R}^{n_b}$ is the vector of identifiable standard parameters; $\boldsymbol{\beta}_{NI} \in \mathbb{R}^{(n_c-n_b)}$ is the vector of non-identifiable standard parameters regrouped with $\boldsymbol{\beta}_I$; and $\mathbf{K} \in \mathbb{R}^{(n_b\times(n_c-n_b))}$ is the matrix of linear regroupings with $\boldsymbol{\beta}_f = \begin{bmatrix}\boldsymbol{\beta}_I^T & \boldsymbol{\beta}_{NI}^T\end{bmatrix}^T$.

Then, according to [30], one has $\boldsymbol{y} = \mathbf{X}_f\boldsymbol{\beta}_f = \mathbf{X}\boldsymbol{\beta}$, and it is evident that the parameters in $\boldsymbol{\beta}_{NI}$ have no impact on the IDM. It follows that some parameters in (19) do not influence the dynamics questioning, therefore, their use as physical constraints. Since the diagonal elements of $\mathbf{I}_j$, m_j, I_{a_j}, f_{v_j} and f_{c_j} must be greater than zero, it is sufficient to use the following constraints

$$\mathbf{A}\boldsymbol{\beta} \succeq \mathbf{0}\,, \tag{27}$$

where $\mathbf{A} \in \mathbb{R}^{(p\times n_b)}$ is a constant matrix selecting the p base parameters that must be greater than zero. We remark that we can write (27) as $\boldsymbol{\beta}_i \geq 0$ for $i = 1,\cdots,p$, and we further assume that $rank(\mathbf{A}) = p$. Since these constraints are physical, they cannot be overly restrictive. Using lower and upper bounds in (27) now is not suggested because such constraints may be overly restrictive. As we will see later, they may deleteriously affect the estimation of $\boldsymbol{\beta}$.

Regarding the criterion, we use the following IV criterion

$$f_0(\boldsymbol{\beta}) = \frac{1}{2}||\mathbf{P}_{\mathbf{Z}}\boldsymbol{\varepsilon}||_2^2\,, \tag{28}$$

proposed in Econometrics. It appears suitable for robot identification because of its geometrical nature. Indeed, we project the error onto the space generated by the instruments, see [37], [40], making it easy to interpret. In [38], chapters 8 and 9, we can find other criteria.

Expanding (28) yields $f_0(\boldsymbol{\beta}) = \frac{1}{2}||\mathbf{P}_{\mathbf{Z}}\boldsymbol{\varepsilon}||_2^2 = \frac{1}{2}\mathbf{y}^T\mathbf{P}_{\mathbf{Z}}\mathbf{y} - \boldsymbol{\beta}^T\mathbf{X}^T\mathbf{P}_{\mathbf{Z}}\mathbf{X}\boldsymbol{\beta} + \frac{1}{2}\boldsymbol{\beta}^T\mathbf{X}^T\mathbf{P}_{\mathbf{Z}}\mathbf{X}\boldsymbol{\beta} = \frac{1}{2}\mathbf{y}^T\mathbf{P}_{\mathbf{Z}}\mathbf{y} - \boldsymbol{\beta}^T\hat{\mathbf{X}}^T\mathbf{y} + \frac{1}{2}\boldsymbol{\beta}^T\hat{\mathbf{X}}^T\mathbf{X}\boldsymbol{\beta} = \frac{1}{2}\boldsymbol{\beta}^T\mathbf{Q}_{ZX}\boldsymbol{\beta} - \mathbf{c}^T\boldsymbol{\beta} + \alpha$, where $\mathbf{Q}_{ZX} = \hat{\mathbf{X}}^T\mathbf{X}$; $\mathbf{c} \in \mathbb{R}^b = \hat{\mathbf{X}}^T\mathbf{y}$; and $\alpha = \frac{1}{2}\mathbf{y}^T\mathbf{P}_{\mathbf{Z}}\mathbf{y}$ is a scalar. The criterion is quadratic to $\boldsymbol{\beta}$ which is unique, see e.g. [31], [32], [47].

Note that one has $\mathbf{Q}_{ZX} \succ \mathbf{0}$. Indeed, $\mathbf{Q}_{ZX} = \mathbf{X}^T\mathbf{Z}(\mathbf{Z}^T\mathbf{Z})^{-1}\mathbf{Z}^T\mathbf{X}$ while it is assumed that $rank\left(\mathbf{Z}^T\mathbf{X}\right) = n_b$ with $\mathbf{Z}^T\mathbf{Z} \succ \mathbf{0}$. Note we do not necessarily assume that $\mathbf{Z} \approx \mathbf{X}_{nf}$ for the derivation. We will discuss this approximation in Section III-G.

C. Problem formulation and intuitive explanation

The problem of physically consistent robot identification is equivalent to an inequality-constrained programming problem formulated as

$$\begin{aligned} &\text{minimize} \quad f_0(\boldsymbol{\beta})\,,\\ &\text{subject to} \quad \mathbf{a}_i^T\boldsymbol{\beta} \geq 0\,,\ \text{for } i = 1,\cdots,p\,, \end{aligned} \tag{29}$$

where $\mathbf{a}_i^T$ is the ith line of $\mathbf{A}$

The Karush – Kuhn – Tucker (KKT) conditions for this problem can be stated as follows: if $\hat{\boldsymbol{\beta}}_{CIV}$, the PC-IDIM estimates of $\boldsymbol{\beta}$, is an optimizer for (29), there exists a multiplier $\hat{\boldsymbol{\mu}} \in \mathbb{R}^p$ such that

$$\begin{aligned} \mathbf{Q}_{ZX}\hat{\boldsymbol{\beta}}_{CIV} - \mathbf{c} + \mathbf{A}^T\hat{\boldsymbol{\mu}} &= \mathbf{0}\,,\\ \hat{\boldsymbol{\beta}}_{CIV_i} &\geq 0\,,\ \text{for } i = 1\cdots p\,,\\ \hat{\mu}_i\hat{\boldsymbol{\beta}}_{CIV_i} &= 0\ \text{for } i = 1\cdots p\,,\\ \hat{\mu}_i &\geq 0\ \text{for } i = 1\cdots p\,. \end{aligned} \tag{30}$$

By introducing the slack variable $\boldsymbol{s} \geq \mathbf{0}$ with $\boldsymbol{s} \in \mathbb{R}^p$, the above conditions can be equivalently formulated as follows

$$\begin{aligned} \mathbf{Q}_{ZX}\hat{\boldsymbol{\beta}}_{CIV} - \mathbf{c} + \mathbf{A}^T\hat{\boldsymbol{\mu}} &= \mathbf{0}\,,\\ \mathbf{A}\hat{\boldsymbol{\beta}}_{CIV} - \hat{\boldsymbol{s}} &= \mathbf{0}\,,\\ \hat{s}_i\hat{\mu}_i &= 0\ \text{for } i = 1\cdots p\,,\\ \hat{s}_i, \hat{\mu}_i &\geq 0\ \text{for } i = 1\cdots p\,. \end{aligned} \tag{31}$$

In [24] chapter 10, and [25], chapter 21, the authors provide an intuitive understanding of (31). The equation (31) shows that the problem becomes nonlinear because of the equation $\hat{s}_i\hat{\mu}_i = 0$ that is called *exclusion* constraint. This term is intuitive since one has $\hat{\mu}_i = 0$ and $\hat{s}_i > 0$ if the constraints are satisfied or $\hat{\mu}_i > 0$ and $\hat{s}_i = 0$ if the constraints are binding, i.e., $\mathbf{A}\hat{\boldsymbol{\beta}}_{CIV} < \mathbf{0}$. Hence, assuming that the constraints are satisfied, we have $\hat{\boldsymbol{\mu}} = \mathbf{0}$ and $\hat{\boldsymbol{s}} > \mathbf{0}$, and (31) reduces to $\mathbf{Q}_{ZX}\hat{\boldsymbol{\beta}}_{CIV} = \mathbf{c}$ which is the unconstrained IV problem. Assuming now that the constraints are not satisfied, we have $\hat{\boldsymbol{\mu}} > \mathbf{0}$ and $\hat{\boldsymbol{s}} = \mathbf{0}$, and (31) reduces to

$$\begin{aligned} \mathbf{Q}_{ZX}\hat{\boldsymbol{\beta}}_{CIV} + \mathbf{A}^T\hat{\boldsymbol{\mu}} &= \mathbf{c}\,,\\ \mathbf{A}\hat{\boldsymbol{\beta}}_{CIV} &= \mathbf{0}\,, \end{aligned} \tag{32}$$

which is the classical equality-constrained IV problem. We will use this intuitive explanation to make the statistical analysis.

In [20]–[22], the author stated that it is not mandatory to detail the problem resolution, while the authors show how the KKT conditions (31) can be viewed as moment conditions in [27]. In this paper, we sketch the resolution to understand how (31) is solved.

D. Problem resolution

An interior-point strategy whose main principles are sketched here to support the resolution of the constraint satisfaction problem described by (30). Indeed, such methods are prevalent and easily accessible through multiple solvers used by CVX [33], [48]. We note that the following approximations $\frac{\partial\mathbf{q}_s}{\partial\boldsymbol{\beta}_f} \approx \mathbf{0}$, $\frac{\partial\dot{\mathbf{q}}_s}{\partial\boldsymbol{\beta}_f} \approx \mathbf{0}$, and $\frac{\partial\ddot{\mathbf{q}}_s}{\partial\boldsymbol{\beta}_f} \approx \mathbf{0}$ that yield $\frac{\partial\mathbf{Z}}{\partial\boldsymbol{\beta}} \approx \mathbf{0}$, [12], hold and this eases the calculation of the KKT conditions.

The strategy is to find the optimal triplet $(\boldsymbol{\beta}, \boldsymbol{\mu}, \boldsymbol{s})$ satisfying the KKT conditions given by (31). First, the nonnegativity constraints are replaced with logarithmic barriers such that $f_0(\boldsymbol{\beta})$ becomes $f_0(\boldsymbol{\beta}) - \zeta\sum_{i=1}^p\log(s_i)$, where ζ is the barrier parameter that usually has a small value. The idea behind the definition of the log barrier is that it is a smooth approximation of the indicator functions, $I_{\{s_i>0\}}(x)$, [32], chapter 11. As $\zeta \to 0$, this approximation becomes closer to the indicator function. Also, for any value of ζ, if any constraints are

violated, the value of the barrier approaches infinity, [32], chapter 11-3. Second, we write the Lagrangian as

$$L_\zeta(\boldsymbol{\beta},\boldsymbol{\mu},\boldsymbol{s}) = f_0(\boldsymbol{\beta}) - \zeta\sum_{i=1}^{p}\log(s_i) - \sum_{i=1}^{p}\mu_i(\mathbf{a}_i^T\boldsymbol{\beta} - s_i)\,, \quad (33)$$

to get the first conditions given by

$$\begin{aligned}\nabla_{\boldsymbol{\beta}} L_\zeta = \partial L_\zeta/\partial\boldsymbol{\beta} &= \mathbf{Q}_{ZX}\boldsymbol{\beta} - \mathbf{c} + \mathbf{A}^T\boldsymbol{\mu} = \mathbf{0}\,,\\ \nabla_{\boldsymbol{\mu}} L_\zeta = \partial L_\zeta/\partial\boldsymbol{\mu} &= \mathbf{A}\boldsymbol{\beta} - \boldsymbol{s} = \mathbf{0}\,,\\ \nabla_{\boldsymbol{s}} L_\zeta = \partial L_\zeta/\partial\boldsymbol{s} &= -\zeta\mathbf{D}_s^{-1}\mathbf{1}_p + \boldsymbol{\mu} = \mathbf{0}\,,\end{aligned} \quad (34)$$

where $\mathbf{D}_s \in \mathbb{R}^{(p\times p)}$ is a diagonal matrix defined by $\mathbf{D}_s = \text{diag}(s_1,\cdots,s_p)$; and $\mathbf{1}_p \in \mathbb{R}^p$ is a vector of ones defined by $\mathbf{1}_p = (1,\cdots,1)^T$. We remark that $\mathbf{D}_s$ is positive-definite since one has $s_i > 0$ for compatibility with the logarithmic barrier. Hence, we write $\mathbf{D}_s \to \mathbf{0}$ and $s_i \to 0$ instead of $\mathbf{D}_s = \mathbf{0}$ and $s_i = 0$ to be consistent with the theory of the logarithmic barrier while adopting the philosophy of [25] chapter 21.

Third, by left multiplying $\nabla_{\boldsymbol{s}} L_\zeta$ by $\mathbf{D}_s$, we obtain the following nonlinear mapping

$$F_\zeta(\boldsymbol{\beta},\boldsymbol{\mu},\boldsymbol{s}) = \begin{bmatrix}\mathbf{Q}_{ZX}\boldsymbol{\beta} + \mathbf{A}^T\boldsymbol{\mu} - \mathbf{c}\\ \mathbf{A}\boldsymbol{\beta} - \boldsymbol{s}\\ \mathbf{D}_s\mathbf{D}_\mu\mathbf{1}_p - \zeta\mathbf{1}_p\end{bmatrix} = \mathbf{0}\,, \quad (35)$$

where $\mathbf{D}_\mu \in \mathbb{R}^{(p\times p)}$ is a diagonal matrix defined by $\mathbf{D}_\mu = \text{diag}(\mu_1,\cdots,\mu_p)$. We note that the difference between (35) and (31) is the presence of $\zeta\mathbf{1}_p$ such that the last equation in (35) represents a perturbed complementarity condition. Consequently, we write $\mathbf{D}_\mu \to \mathbf{0}$ and $\mu_i \to 0$ (resp. $\mathbf{D}_s \to \mathbf{0}$ and $s_i \to 0$) instead of $\mathbf{D}_\mu = \mathbf{0}$ and $\mu_i = 0$ (resp. $\mathbf{D}_s = \mathbf{0}$ and $s_i = 0$).

The idea is to apply Newton's method to (35) to compute the optimal triplet $(\hat{\boldsymbol{\beta}}_{CIV},\hat{\boldsymbol{\mu}},\hat{\boldsymbol{s}})$ on the central path, and automatically compute ζ with $\zeta = \varsigma\kappa$ where $\varsigma \in [0,1]$ is a parameter chosen by the algorithm, and κ is a duality measure introduced later, [32]. At iteration k, the Newton increments $(\Delta\hat{\boldsymbol{\beta}}_{CIV}^{(k)},\Delta\hat{\boldsymbol{\mu}}^{(k)},\Delta\hat{\boldsymbol{s}}^{(k)})$ are the solution of the linear system obtained from the linearization of (35) around the current estimates $(\hat{\boldsymbol{\beta}}_{CIV}^{(k-1)},\hat{\boldsymbol{\mu}}^{(k-1)},\hat{\boldsymbol{s}}^{(k-1)})$,

$$\begin{bmatrix}\mathbf{Q}_{ZX} & \mathbf{A}^T & \mathbf{0}\\ \mathbf{A} & \mathbf{0} & \mathbf{I}_p\\ \mathbf{0} & \mathbf{D}_s & \mathbf{D}_\mu\end{bmatrix}\begin{bmatrix}\Delta\boldsymbol{\beta}_{CIV}^{(k)}\\ \Delta\boldsymbol{\mu}^{(k)}\\ \Delta\boldsymbol{s}^{(k)}\end{bmatrix} = \begin{bmatrix}-\mathbf{r}_c\\ -\mathbf{r}_b\\ \mathbf{g}_s\end{bmatrix} \quad (36)$$

where $\mathbf{r}_c = \mathbf{Q}_{ZX}\hat{\boldsymbol{\beta}}_{CIV}^{(k-1)} + \mathbf{A}^T\hat{\boldsymbol{\mu}}^{(k-1)} - \mathbf{c}$; $\mathbf{r}_b = \mathbf{A}\hat{\boldsymbol{\beta}}_{CIV}^{(k-1)} - \hat{\boldsymbol{s}}^{(k-1)}$; and $\mathbf{g}_s = \mathbf{D}_s\mathbf{D}_\mu\mathbf{1}_p - \varsigma\kappa\mathbf{1}_p$.

To resolve (35), it is preferable to stick to the philosophy adopted in [25] chapter 21 because it is helpful for statistical analysis. However, this approach is similar to the resolution detailed in [32], chapters 10 and 11.

First, we remark that the Jacobian matrix on the left-hand side of (36) is full rank, [32], chapter 11. Indeed, we have $rank(\mathbf{Q}_{ZX}) = n_b$ because of (10), one has $rank(\mathbf{A}) = p$ by assumption, and $\mathbf{D}_s$, $\mathbf{D}_\mu$ are full rank because of the logarithmic barrier. Second, $(\Delta\hat{\boldsymbol{\beta}}_{CIV}^{(k)},\Delta\hat{\boldsymbol{\mu}}^{(k)},\Delta\hat{\boldsymbol{s}}^{(k)})$ are calculated with

$$\begin{bmatrix}\Delta\hat{\boldsymbol{\beta}}_{CIV}^{(k)}\\ \Delta\hat{\boldsymbol{\mu}}^{(k)}\\ \Delta\hat{\boldsymbol{s}}^{(k)}\end{bmatrix} = \begin{bmatrix}\mathbf{Q}_{ZX} & \mathbf{A}^T & \mathbf{0}\\ \mathbf{A} & \mathbf{0} & \mathbf{I}_p\\ \mathbf{0} & \mathbf{D}_s & \mathbf{D}_\mu\end{bmatrix}^{-1}\begin{bmatrix}-\mathbf{r}_c\\ -\mathbf{r}_b\\ \mathbf{g}_s\end{bmatrix} \quad (37)$$

To compute κ in (36), we recall that the set of points $(\boldsymbol{\beta},\boldsymbol{\mu},\boldsymbol{s})$ satisfying $F_\zeta(\boldsymbol{\beta},\boldsymbol{\mu},\boldsymbol{s}) = \mathbf{0}$, for some ζ, is called the central path, [32] chapter 11. The new iterate is given by $(\hat{\boldsymbol{\beta}}_{CIV}^{(k)},\hat{\boldsymbol{\mu}}^{(k)},\hat{\boldsymbol{s}}^{(k)}) = (\hat{\boldsymbol{\beta}}_{CIV}^{(k-1)},\hat{\boldsymbol{\mu}}^{(k-1)},\hat{\boldsymbol{s}}^{(k-1)}) + \gamma(\Delta\hat{\boldsymbol{\beta}}_{CIV}^{(k)},\Delta\hat{\boldsymbol{\mu}}^{(k)},\Delta\hat{\boldsymbol{s}}^{(k)})$, with γ chosen such that $(\hat{\boldsymbol{\beta}}_{CIV}^{(k)},\hat{\boldsymbol{\mu}}^{(k)},\hat{\boldsymbol{s}}^{(k)})$ stays feasible. Given a feasible iterate we calculate the duality measure κ with, [32],

$$\kappa = \frac{(\hat{\boldsymbol{s}}^{(k)})^T\hat{\boldsymbol{\mu}}^{(k)}}{p}, \quad (38)$$

Finally, this process is iterated until its convergence.

E. Relationship with [25] chapter 21

The equations (35), (36) and (37) emphasize how the constrained IV problem is resolved. From initial values $(\boldsymbol{\beta}_{CIV}^{(0)},\boldsymbol{\mu}^{(0)},\boldsymbol{s}^{(0)})$, we compute increments so that the problem remains feasible. We solve the exclusion constraint with the logarithmic barrier. If $\hat{s}_i \to 0$, then the barrier, and so the Lagrangian multiplier $\hat{\mu}_i$, is activated and one gets $\hat{\beta}_{CIV_i} \to 0$. If $\hat{s}_i > 0$, the barrier, and so the Lagrangian multiplier $\hat{\mu}_i$, is deactivated, and one obtains $\hat{\beta}_{CIV_i} > 0$. This is consistent with the analysis made in [25], chapter 21.

We can pursue further the links with [25], chapter 21. First, if the inequality constraints are all satisfied, $\mathbf{D}_\mu \to \mathbf{0}$, $\mathbf{D}_s \succ \mathbf{0}$ and $\Delta\hat{\boldsymbol{\mu}}^{(k)} \to \mathbf{0}$ follows because of the third line of (36), while the second line tells that $\mathbf{A}\hat{\boldsymbol{\beta}}_{CIV}^{(k-1)} = \hat{\boldsymbol{s}}^{(k-1)}$. Then, with the first line of (36), one finally gets $\mathbf{Q}_{ZX}\Delta\boldsymbol{\beta}_{CIV}^{(k)} = -\mathbf{r}_c$ which is the unconstrained IV solved with the Gauss-Newton algorithm, see e.g., [31] and [28]. So, we retrieve the unconstrained IV problem. Second, if the inequality constraints are not satisfied, $\mathbf{D}_s \to \mathbf{0}$, $\mathbf{D}_\mu \succ \mathbf{0}$ and $\Delta\hat{\boldsymbol{s}}^{(k)} \to \mathbf{0}$ follows because of the third line of (36). Then, with the first and second lines of (36), one finally gets

$$\begin{bmatrix}\mathbf{Q}_{ZX} & \mathbf{A}^T\\ \mathbf{A} & \mathbf{0}\end{bmatrix}\begin{bmatrix}\Delta\boldsymbol{\beta}_{CIV}^{(k)}\\ \Delta\boldsymbol{\mu}^{(k)}\end{bmatrix} = \begin{bmatrix}-\mathbf{r}_c\\ -\mathbf{r}_b\end{bmatrix} \quad (39)$$

which is the IV estimation under equality constraints solved by a Gauss-Newton algorithm, see [32], chapter 10.

To conclude this subsection, we consider constraints such that $h_i(\beta) \geq 0,\ for\ i = 1\cdots p$, where each h_i is a function twice-differentiable. We must substitute $\mathbf{Q}_{ZX}$ by $\mathbf{H}_{kkt} = \mathbf{Q}_{ZX} + \sum_{i=1}^{p}\mu_i\nabla^2_{\boldsymbol{\beta}}h_i(\hat{\boldsymbol{\beta}}_{CIV}^{(k-1)})$ where $\nabla^2_{\boldsymbol{\beta}}h_i(\hat{\boldsymbol{\beta}}_{CIV}^{(k-1)}) \in \mathbb{R}^{(n_b\times n_b)}$ is the Hessian matrix of $h_i(\boldsymbol{\beta})$ evaluated at $\hat{\boldsymbol{\beta}}_{CIV}^{(k-1)}$ in the left-hand side matrix in (36). Proving that this matrix is still invertible is straightforward. Indeed, we have $\mathbf{Q}_{ZX} \succ \mathbf{0}$ because $rank\left(\mathbf{Z}^T\mathbf{X}\right) = n_b$, and $\nabla^2_{\boldsymbol{\beta}}h_i(\hat{\boldsymbol{\beta}}_{CIV}^{(k-1)}) \succ \mathbf{0}$ by definition of a Hessian matrix, [32] chapter 10. Then, it follows straight that $\mathbf{H}_{kkt} \succ \mathbf{0}$ by addition of two positive-definitive matrices, see [32], chapter 11.

F. Consistency of PC-IDIM-IV estimates

To make the consistency analysis, we assume that the algorithm has converged which means the problem is feasible. Since $\mathbf{q}, \dot{\mathbf{q}}, \ddot{\mathbf{q}}$ are quasi-stationary signals whose the first four moments are finite, then $\text{plim}_{r\to\infty}\left(\frac{1}{r}\mathbf{Q}_{ZX}\right)$ exists and is finite, [13], [37], chapter 7, and, [38], chapter 8. We further assume that (10) holds and there is no modeling error. Let $\hat{\boldsymbol{\beta}}_{CIV}$, $\hat{\boldsymbol{\mu}}$ and $\hat{\boldsymbol{s}}$ the estimates of $\boldsymbol{\beta}$, $\boldsymbol{\mu}$ and $\boldsymbol{s}$, respectively, obtained after the algorithm convergence.

If the constraints are satisfied, i.e., $\mathbf{A}\hat{\boldsymbol{\beta}}_{CIV} \succ \mathbf{0}$, then $\hat{\boldsymbol{\mu}} \to \mathbf{0}$, and one has $\hat{\boldsymbol{\beta}}_{CIV} = \hat{\boldsymbol{\beta}}_{IV}$, and so $\text{plim}_{r\to\infty}\left(\hat{\boldsymbol{\beta}}_{CIV}\right) = \text{plim}_{r\to\infty}\left(\hat{\boldsymbol{\beta}}_{IV}\right) = \boldsymbol{\beta}$. This is consistent with the result exposed in [25], chapter 21. This result is unsurprising since the IDIM-IV estimates satisfy the physical constraints if they are consistent, [12], [19].

If the constraints are binding, the IV estimation under inequality constraints turns to the IV estimation under equality constraints. It comes out that the PC-IDIM-IV estimates are given by

$$\hat{\boldsymbol{\beta}}_{CIV} = \begin{bmatrix} \mathbf{0} \\ \left(\mathbf{Z}_U^T\mathbf{X}_U\right)^{-1}\mathbf{Z}_U^T\mathbf{y} \end{bmatrix}, \tag{40}$$

where $\mathbf{X}_U \in \mathbb{R}^{(r\times(n_b-p))}$ (resp. $\mathbf{Z}_U \in \mathbb{R}^{(r\times(n_b-p))}$) are the $n_b - p$ columns of $\mathbf{X}$ (resp. $\mathbf{Z}$) related to the $n_b - p$ unconstrained parameters; see [24] chapter 10 and [25] chapter 21. From (40), it is clear that $\hat{\boldsymbol{\beta}}_{CIV} \neq \hat{\boldsymbol{\beta}}_{IV}$, and so $\text{plim}_{r\to\infty}\left(\hat{\boldsymbol{\beta}}_{CIV}\right) \neq \boldsymbol{\beta}$.

To pursue further this analysis, [25], chapter 21, shows that we can relate $\hat{\boldsymbol{\beta}}_{CIV}$ and $\hat{\boldsymbol{\beta}}_{IV}$. Let $\hat{\boldsymbol{\beta}}_{IV}^{C}$ the p unconstrained IV estimates related to the p constraints, and let $\hat{\boldsymbol{\beta}}_{IV}^{U}$ the $n_b - p$ remaining unconstrained IV estimates. One has

$$\hat{\boldsymbol{\beta}}_{CIV} = \begin{bmatrix} \hat{\boldsymbol{\beta}}_{CIV}^{C} \\ \hat{\boldsymbol{\beta}}_{CIV}^{U} \end{bmatrix} = \begin{bmatrix} \mathbf{0} \\ \hat{\boldsymbol{\beta}}_{IV}^{U} + \left(\mathbf{Z}_U^T\mathbf{X}_U\right)^{-1}\mathbf{Z}_U^T\mathbf{X}_C\hat{\boldsymbol{\beta}}_{IV}^{C} \end{bmatrix}, \tag{41}$$

where $\hat{\boldsymbol{\beta}}_{CIV}^{C}$ (resp. $\hat{\boldsymbol{\beta}}_{CIV}^{U}$) are the p PC-IDIM-IV estimates related to the p constrained (resp. $n_b - p$ unconstrained) parameters; $\mathbf{X}_C \in \mathbb{R}^{(r\times p)}$ is the p columns of $\mathbf{X}$ related to the p constrained parameters; see [25], chapter 21. It follows that $\hat{\boldsymbol{\beta}}_{CIV}^{U} \neq \hat{\boldsymbol{\beta}}_{IV}^{U}$ unless the the columns of $\mathbf{X}_C$ are orthogonal to $\mathbf{Z}_U$. A short justification of (41) is given in appendix VI-D. Interestingly, (41) shows that the estimation under equality constraints turns into an omitted variable bias. Indeed, if the inequality constraints are binding, then the initial constrained problem turns into a procedure with equality constraints which is equivalent to fixing some parameters at $\mathbf{0}$ in our case. These fixed parameters are, thus, missing in the IDM, and it is an omitted-variable bias problem.

G. Covariance matrix of PC-IDIM-IV estimates

Concerning the covariance matrix of $\hat{\boldsymbol{\beta}}_{CIV}$, as stated in [38], chapter 8, we can write

$$\hat{\boldsymbol{\Sigma}}_{CIV} = \hat{\boldsymbol{\Sigma}}_{2SLS} = \left(\hat{\mathbf{X}}^T\hat{\boldsymbol{\Omega}}^{-1}\hat{\mathbf{X}}\right)^{-1}, \tag{42}$$

with $\hat{\boldsymbol{\Sigma}}_{CIV} \succeq \boldsymbol{\Sigma}_{IV}^{opt}$, [38], chapter 8. Consequently, we can conclude from (42)

$$\sqrt{r}\left(\hat{\boldsymbol{\beta}}_{CIV} - \boldsymbol{\beta}\right) \overset{a}{\sim} \mathcal{N}\left(\mathbf{0}, \text{plim}_{r\to\infty}\left(\frac{\hat{\mathbf{X}}^T\boldsymbol{\Omega}^{-1}\hat{\mathbf{X}}}{r}\right)^{-1}\right), \tag{43}$$

where $\mathcal{N}$ is the normal distribution.

We now discuss the implications of $\mathbf{Z} \approx \mathbf{X}_{nf}$. First, one gets, $E(\hat{\mathbf{X}}) = E\left(\mathbf{P}_{\mathbf{Z}}\mathbf{X}\right) \approx \mathbf{X}_{nf}$, $E\left(\hat{\mathbf{X}}^T\mathbf{X}\right) \approx \mathbf{X}_{nf}^T\mathbf{X}_{nf}$ and $E\left(\mathbf{Z}^T\mathbf{X}\right) \approx \mathbf{X}_{nf}^T\mathbf{X}_{nf}$. It follows that the IV and 2SLS estimates have the same asymptotic covariance matrix, and so $\sqrt{r}\left(\hat{\boldsymbol{\beta}}_{CIV} - \boldsymbol{\beta}\right) \overset{a}{\sim} \sqrt{r}\left(\hat{\boldsymbol{\beta}}_{IV} - \boldsymbol{\beta}\right)$, and this result agrees with the theory exposed in [38], chapter 8. Second, $\boldsymbol{\Pi} \approx \mathbf{I}_{b_e}$, where $\mathbf{I}_{b_e}$ is the $(n_b \times n_b)$ identity matrix, follows. To validate or invalidate the hypothesis $\hat{\boldsymbol{\Pi}} = \mathbf{I}_{b_e}$, the authors introduced a statistic in [49]. Since we use the DDM to construct $\mathbf{Z}$ and the IDM to estimate $\boldsymbol{\beta}$, it is natural to expect that $\mathbf{Z} \approx \mathbf{X}_{nf}$ for robot identification, otherwise, it means that we identify $\boldsymbol{\beta}$ with significant modeling errors.

It comes out that $\mathbf{Z} \approx \mathbf{X}_{nf}$, or equivalently $\boldsymbol{\Pi} \approx \mathbf{I}_{b_e}$, is crucial to constructing the *optimal* instrumental matrix.

We have conducted Monte Carlo simulations as in [19] to validate (42). The results being the same as those reported in [19], they show that (42) is correct and consistent with the analysis of [24], chapter 10, and [25], chapter 21. They also show that the IV estimates are *near* optimal when $\mathbf{Z} \approx \mathbf{X}_{nf}$.

When the constraints are biding, the PC-IDIM-IV estimates are biased and there is little interest in calculating the covariance matrix.

H. Overly restrictive constraints

The case of overly restrictive constraints is now discussed. By *overly restrictive constraints* it is understood that $\boldsymbol{\beta}$ lies *outside* of the accessible space of solutions. $\boldsymbol{\beta}$ being unique because the problem is linear to $\boldsymbol{\beta}$, it is impossible that $\hat{\boldsymbol{\beta}}_{CIV}$ converges to *another* local minimal, [32], [37]. In this case, it is evident that $\hat{\boldsymbol{\beta}}_{CIV}$ is biased. Two outcomes are possible: the problem is unfeasible or the algorithm converges.

If the problem is unfeasible, the constraints cannot be satisfied, the algorithm cannot compute a valid κ with (38) and is aborted. There is no $\hat{\boldsymbol{\beta}}_{CIV}$ and users must rework constraints or the IDM.

If the algorithm succeeds in converging despite overly restrictive constraints, it means it succeeded in computing a valid κ with (38). Since we have emphasized that $\hat{\boldsymbol{\beta}}_{CIV}$ is a consistent estimate of $\boldsymbol{\beta}$ if and only if $\hat{\boldsymbol{\mu}} \to \mathbf{0}$, it is, therefore, enough to run the PC-IDIM-IV algorithm and check that $\hat{\boldsymbol{\mu}} \to \mathbf{0}$ holds. It is also possible to compute the norm of the gradient of the IV method given by $\mathbf{g}_{IV} = \mathbf{Z}^T\left(\mathbf{y} - \mathbf{X}\hat{\boldsymbol{\beta}}_{CIV}\right)$ which must be null, i.e., less than 10^{-8} in practice, see [32]. If $E\left(\hat{\boldsymbol{\beta}}_{CIV}\right) \neq \boldsymbol{\beta}$, it is evident that $\mathbf{g}_{IV} \neq \mathbf{0}$. However, this is a criterion and not a formal proof.

Overly restrictive constraints may occur when using lower and upper bounds in (27). The statistical analysis presented in the previous subsection enlightened why we must not use them while identifying $\boldsymbol{\beta}$. Indeed, if the constraints are binding, then

the constrained parameters are fixed to their boundary values so that (40) becomes, [25] chapter 21,

$$\hat{\boldsymbol{\beta}}_{CIV} = \begin{bmatrix} \mathbf{d} \\ \left(\mathbf{Z}_U^T \mathbf{X}_U\right)^{-1} \mathbf{Z}_U^T \left(\mathbf{y} - \mathbf{X}_C \mathbf{d}\right) \end{bmatrix}, \tag{44}$$

where $\mathbf{d} \in \mathbb{R}^p$ is the vector of lower or upper bounds. By relating $\hat{\boldsymbol{\beta}}_{CIV}$ and $\hat{\boldsymbol{\beta}}_{IV}$, one finally obtains

$$\hat{\boldsymbol{\beta}}_{CIV} = \begin{bmatrix} \hat{\boldsymbol{\beta}}_{CIV}^C \\ \hat{\boldsymbol{\beta}}_{CIV}^U \end{bmatrix} = \begin{bmatrix} \mathbf{d} \\ \hat{\boldsymbol{\beta}}_{IV}^U + \left(\mathbf{Z}_U^T \mathbf{X}_U\right)^{-1} \mathbf{Z}_U^T \mathbf{X}_C \left(\hat{\boldsymbol{\beta}}_{IV}^C - \mathbf{d}\right) \end{bmatrix}. \tag{45}$$

We evidently have $\hat{\boldsymbol{\beta}}_{CIV}^U \neq \hat{\boldsymbol{\beta}}_{IV}^U$ unless the the columns of $\mathbf{X}_C$ are orthogonal to $\mathbf{Z}_U$ or $\hat{\boldsymbol{\beta}}_{CIV}^C = \mathbf{d}$, which is unlikely to occur. We sketch a short justification of (45) in appendix VI-D.

I. PC-IDIM-IV algorithm

This subsection summarizes the PC-IDIM-IV algorithm illustrated in Fig. 1.

iteration 0: Collect $\mathbf{q}$ and $\boldsymbol{\tau}$, compute $\hat{\mathbf{q}}, \hat{\dot{\mathbf{q}}}, \hat{\ddot{\mathbf{q}}}$, then construct $\boldsymbol{y}$ and $\mathbf{X}\left(\hat{\mathbf{q}}, \hat{\dot{\mathbf{q}}}, \hat{\ddot{\mathbf{q}}}\right)$. Initialize the PC-IDIM-IV algorithm with the computer-aided-design (CAD) values of $\boldsymbol{\beta}$.

iteration it: Construct $\mathbf{Z}$ by simulating the DDM and $\hat{\boldsymbol{\beta}}_{CIV}^{(k-1)}$, the PC-IDIM-IV estimates calculated at the previous iteration. Then, compute $\hat{\boldsymbol{\beta}}_{CIV}^{(k)}$ by minimizing $f_0(\boldsymbol{\beta})$ defined by (28) subject to the constraints given by (27). Run this iterative algorithm until convergence, i.e.,

$$\frac{|\hat{\boldsymbol{\beta}}_{CIV}^{(k)}(i) - \hat{\boldsymbol{\beta}}_{CIV}^{(k-1)}(i)|}{|\hat{\boldsymbol{\beta}}_{CIV}^{(k)}(i)|} < tol_\beta\,, \tag{46}$$

where $\hat{\boldsymbol{\beta}}_{CIV}^{(k)}(i)$ is the i-th component of $\hat{\boldsymbol{\beta}}_{CIV}^{(k)}$; and tol_β is a user-defined threshold.

final iteration: Consider $\hat{\boldsymbol{\beta}}_{CIV}$, and compute the covariance matrix of the PC-IDIM-IV estimates with (42).

PC-IDIM-IV consists of two nested iterative algorithms: the outer one which focuses on the convergence of the PC-IDIM-IV estimates, equation (46); and the inner one that accounts for the physical constraints solved by a Gauss-Newton algorithm, equations (37). Experimental results will show that this approach is not very time-consuming.

IV. Experimental validation

A. Robotic manipulator, exciting trajectories and data acquisition

The TX40 robot has a serial structure with six rotational joints and is characterized by a coupling between the joints 5 and 6, see [12]. It is controlled by a cascade controller, which consists of a P control of the inner velocity loop and a P control of the outer position loop. The bandwidth of the first (resp. last) three position closed loops is 10Hz (resp. 20 Hz).

For the experimental validation of the PC-IDIM-IV method and the comparison with the other procedures, the references $\mathbf{q}_r, \dot{\mathbf{q}}_r, \ddot{\mathbf{q}}_r$ consist of smoothed bang-bang trajectories. They provide a condition number of 200 for $\mathbf{X}$, which is good to avoid numerical issues, [50]. All the data are stored with a sampling rate $f_m = 5kHz$. To validate the estimates, we have carried out cross-validations with three fifth-order polynomials passing through points different from those of the trajectories used for identification. The cross-validation data are stored with a different sampling rate given by $f_m^{cv} = 1kHz$.

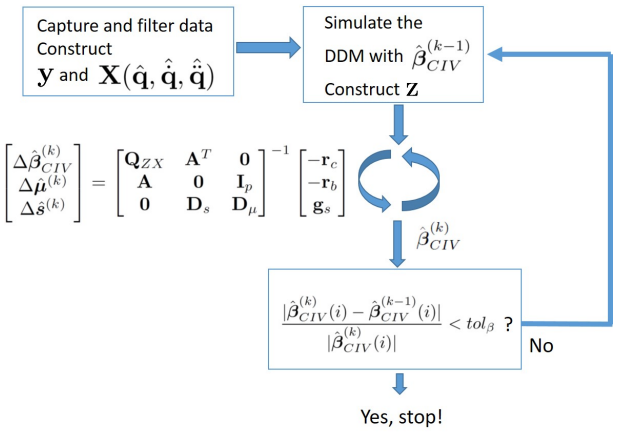

Fig. 1. Principle of the PC-IDIM-IV method

We investigate five scenarios: one with actual data, a second one with downgraded data, the third one with overly restrictive constraints, a fourth one with an error in $C_j(s)$, and the last one with an IDM error. Data are stored with a sampling rate $f_m = 5kHz$. We filter data for all scenarios and methods according to the process described in [10].

Finally, all the simulations are executed on a laptop equipped with an Intel Core i5-10400H processor, 16.0 GB of RAM (DDR4 SDRAM technology), and a capacity of 500 GB. MATLAB version 2019-B is used.

B. First scenario: actual data

With actual data, IDIM-IV, DIDIM, PC-IDIM-IV, and PC-DIDIM converge in 5 iterations. For any method, the DDM simulation for an 8s trajectory and the calculation of the estimates need 5s. From this, the Gauss-Newton algorithm needs 13 iterations to converge and takes 3s. So, IDIM-IV and DIDIM converge in 25 seconds, while PC-IDIM-IV and PC-DIDIM converge in 40 seconds, which is acceptable.

The results obtained with the direct comparisons are given in Table I, while the results of the cross-test validations are given in Table II. We recall that the relative errors are calculated with $rel_{err} = 100 \cdot ||\mathbf{y} - \mathbf{X}\hat{\boldsymbol{\beta}}||/||\mathbf{y}||$, where $\hat{\boldsymbol{\beta}}$ is the estimate provided by the method.

The results gathered in Tables I and II show that the relative errors do not vary significantly. Furthermore, the cross-validation for the first joint with the first trajectory illustrated in Fig. 2 shows that the torque reconstructed with the PC-IDIM-IV estimates fits the actual one. We obtain plots similar to those of the other methods. Using an IV approach and the physical constraints do not significantly improve the results when the actual data, a good model, and appropriate data filtering are employed. This result is consistent with those previously published in [10], [12], [19]. In this case, we have $\mathbf{X} \approx \mathbf{Z} \approx \mathbf{X}_{nf}$, yielding PC-IDIM-LS, PC-IDIM-IV, and PC-DIDIM estimates that are close to each other.

TABLE I
RELATIVE ERRORS OBTAINED WITH DIRECT COMPARISONS - ACTUAL DATA

Joint j	IDIM-LS	IDIM-IV	DIDIM
1	5.2%	5.4%	5.5%
2	5.0%	5.3%	5.3%
3	5.0%	5.1%	5.1%
4	5.6%	5.7%	5.8%
5	7.2%	7.2%	7.2%
6	7.1%	7.5%	7.5%
Joint j	PC-IDIM-LS	PC-IDIM-IV	PC-DIDIM
1	5.2%	5.4%	5.5%
2	5.0%	5.3%	5.3%
3	5.0%	5.1%	5.1%
4	5.6%	5.7%	5.8%
5	7.2%	7.2%	7.2%
6	7.1%	7.5%	7.5%

TABLE II
RELATIVE ERRORS OBTAINED WITH CROSS-VALIDATION - ACTUAL DATA

Traj.	IDIM-LS	IDIM-IV	DIDIM
1	6.1%	6.4%	6.4%
2	6.3%	6.8%	6.8%
3	6.7%	7.0%	7.1%
Traj.	PC-IDIM-LS	PC-IDIM-IV	PC-DIDIM
1	6.1%	6.4%	6.4%
2	6.3%	6.8%	6.8%
3	6.7%	7.0%	7.1%

Interestingly, if we estimate $\mathbf{\Pi}$ with (21), the statistics presented in [49] accepts the hypothesis $\hat{\mathbf{\Pi}} = \mathbf{I}_{n_b}$.

C. Second scenario: downgraded data

Now, we downgrade position data from 2e-4 degrees per count to 2e-2 degrees per count. This can occur when robots operate in hostile or perturbed environments, [51]. With downgraded data, PC-IDIM-IV and IDIM-IV converge in 7 iterations, while PC-DIDIM converges in 6 iterations. In this configuration, the methods converge in less than 1 minute, which is acceptable.

From the relative errors obtained with direct and cross-validations gathered in Tables III and IV, we see that the PC-IDIM-LS estimates are no longer consistent, whereas PC-IDIM-IV, IDIM, and PC-DIDIM estimates remain consistent. Indeed, the relative errors are still below 10%, whereas they are higher than 20% for PC-IDIM-LS. Besides, the torque reconstruction with the PC-IDIM-IV estimates illustrated in Fig. 3 with the first joint and the first trajectory shows that the fitting is excellent despite a noisier signal.

This result is consistent with those exposed in [10], [12], [19]. When the noise is too high, the bias of the LS estimator is no longer negligible in practice. Adding the physical constraints does not remove the persisting bias. IDIM-IV, PC-IDIM-IV, DIDIM, and PC-DIDIM are immune to this correlation because the fundamental relation $\text{plim}_{r\to\infty}\left(\frac{1}{r}\mathbf{Z}^T\boldsymbol{\varepsilon}\right) = \mathbf{0}$ holds.

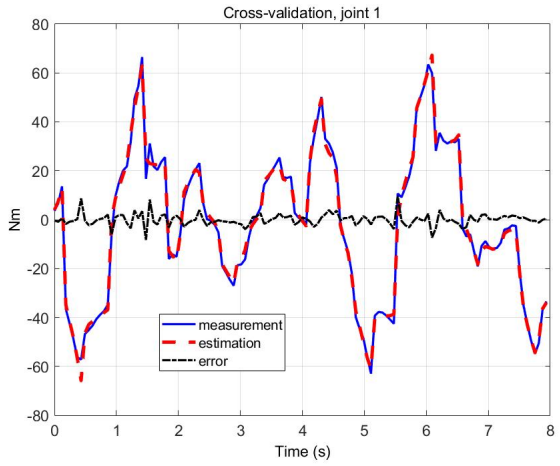

Fig. 2. Cross-validation, first joint and first trajectory, actual data.

TABLE III
RELATIVE ERRORS OBTAINED WITH DIRECT COMPARISONS - DOWNGRADED DATA

Joint j	IDIM-LS	IDIM-IV	DIDIM
1	25.3%	6.1%	6.1%
2	24.7%	5.9%	6.0%
3	25.2%	6.0%	6.1%
4	25.8%	5.9%	5.9%
5	27.5%	8.0%	8.0%
6	28.0%	8.1%	8.2%
Joint j	PC-IDIM-LS	PC-IDIM-IV	PC-DIDIM
1	25.3%	6.1%	6.1%
2	24.7%	5.9%	6.0%
3	25.2%	6.0%	6.1%
4	25.8%	5.9%	5.9%
5	27.5%	8.0%	8.0%
6	28.0%	8.1%	8.2%

TABLE IV
RELATIVE ERRORS OBTAINED WITH CROSS-VALIDATION - DOWNGRADED DATA

Traj.	IDIM-LS	IDIM-IV	DIDIM
1	26.4%	7.1%	7.2%
2	26.5%	7.6%	7.6%
3	27.8%	7.9%	8.0%
Traj.	PC-IDIM-LS	PC-IDIM-IV	PC-DIDIM
1	26.4%	7.1%	7.2%
2	26.5%	7.6%	7.6%
3	27.8%	7.9%	8.0%

D. Third scenario: overly restrictive constraints and constraints given by (19)

We analyze the effects of overly restrictive constraints. To do so, we impose lower and upper bounds to estimates, i.e., we modify (27) by $\beta_{L_j} \leq \beta_j \leq \beta_{U_j}$, where β_{L_j} and β_{U_j} are the lower and upper bounds of β_j, respectively. We tune the bounds so that $\boldsymbol{\beta}$ lies outside of the accessible space of solutions and the problem remains feasible. For instance, if $\beta_j = 1.0$, we choose $\beta_{L_j} = 0.8$ and $\beta_{U_j} = 0.9$. Actual data are used. The performances are the same as those we show in subsection IV-B; PC-IDIM-IV and PC-DIDIM converge in 40 seconds. Interestingly, all the $\hat{\beta}_j$'s stick to their lower or upper bounds while $\hat{\mu}_j \neq 0$. This means that the constraints are binding and so, they are overly restrictive. Besides, by applying (45), we retrieve the PC-IDIM-IV estimates from the IDIM-IV estimates. These results support the analysis presented in the subsections III-F and III-H.

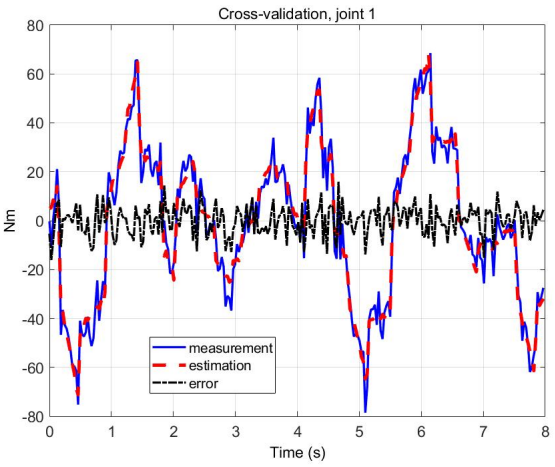

Fig. 3. Cross-validation, first joint, and first trajectory with downgraded data.

We show now that the constraints given by (19) and used in [14], [15], [17], [19] do not bring additional information compared to the constraints (27). To do so, we include $\hat{\boldsymbol{\beta}}_{CIV}$ as inequality constraints so that the constrained problem becomes

$$\begin{aligned} \text{minimize} \quad & \frac{1}{2}||\mathbf{P}_{\mathbf{Z}}\left(\mathbf{y}-\mathbf{X}_f\boldsymbol{\beta}_f\right)||_2^2, \\ \text{subject to} \quad & h_i(\boldsymbol{\beta}_f) \geq 0\,, \text{ for } i=1,\cdots,p\,, \\ & \underline{\beta}_j \leq \beta_j \leq \overline{\beta}_j\,, \text{ for } j=1,\cdots,n_b\,, \end{aligned} \tag{47}$$

where $\beta_j = \beta_{I_j} + \mathbf{K}_j^T\boldsymbol{\beta}_{NI}$ with $\mathbf{K}_j^T$ is the j-th line of $\mathbf{K}$ defined in (26); $\underline{\beta}_j = \hat{\beta}_{CIV_j} - 3\cdot\hat{\sigma}_j$ and $\overline{\beta}_j = \hat{\beta}_{CIV_j} + 3\cdot\hat{\sigma}_j$ where $\hat{\sigma}_j = \sqrt{\hat{\boldsymbol{\Sigma}}_{CIV}(j,j)}$ is the estimated standard deviation of $\hat{\boldsymbol{\beta}}_{CIV_j}$. Equation (47) shows we search a constrained estimate $\hat{\boldsymbol{\beta}}_f$ so that $\hat{\boldsymbol{\beta}} = [\mathbf{I}_{n_b}\mathbf{K}]\,\hat{\boldsymbol{\beta}}_f$ lies within the $+/-3\hat{\sigma}$ bandwidth centered in $\hat{\boldsymbol{\beta}}_{CIV}$. Note that in [14] and [17], the authors used equality constraints to check the physical feasibility of IDIM-LS estimates and it is not correct. Indeed, we know that estimates are stochastic and not deterministic quantities. It is, therefore, unlikely that an estimate fits *exactly* a deterministic value. It would have been correct to treat $\hat{\boldsymbol{\beta}}_{IV}$ as a stochastic constraint as done in [20]–[22], [25], [27].

The problem (47) is feasible since PC-IDIM-IV and PC-DIDIM converge in 5 iterations. Let $\hat{\boldsymbol{\beta}}_{DCIV}$ the estimates obtained with (47). The DDM simulation needs 5s, the Gauss-Newton algorithm needs 20 iterations to converge in 5s, and it follows that PC-IDIM-IV and PC-DIDIM converge in 45 seconds. The increase of the time computing is explained by the $2\cdot n_b$ inequality constraints we have added. The differences observed between $\hat{\boldsymbol{\beta}}_{DCIV}$ and $\hat{\boldsymbol{\beta}}_{CIV}$ lie within the $+/-3\cdot\hat{\sigma}_j$ band and we can write $\hat{\boldsymbol{\beta}}_{DCIV} \approx \hat{\boldsymbol{\beta}}_{CIV}$ according to the theory of system identification, see, e.g. [37], [40]. This result proves that the constraints (27) are enough and are equivalent to (19).

To conclude this part, if we use equality constraints, i.e., $\beta_j = \hat{\beta}_{CIV_j}$, in (47) instead of inequality constraints, the problem becomes infeasible. It is an expected outcome since we have treated an estimate as a deterministic value, whereas it is not. This is the point the authors have missed in [14] and [17].

E. Fourth scenario: error in the controller

We introduce errors located in $C_j(s)$ to evaluate the robustness of PC-IDIM-IV against modeling errors. As in most cases, industrials do not share it unless with formal agreements; we must identify it. We downgrade the gains of the simulated control so that the bandwidth of the first (resp. last) three joints is 5Hz (resp. 10Hz). Loosely speaking, we divide the bandwidth of the position closed loops by two.

With such errors, PC-IDIM-IV, IDIM-IV, and PC-DIDIM converge in 5 iterations, whereas DIDIM fails to converge. Again, for an 8s trajectory, the simulation of the DDM takes 5s. IDIM-IV takes 25 seconds for convergence. The GN algorithm converges in 13 iterations in 3s. So, PC-IDIM-IV and PC-DIDIM converge in less than 1 minute. Such errors do not affect the running time of algorithms. The relative errors gathered in Table V and Table VI show that IDIM-IV and PC-IDIM-IV perform well despite errors in $C_j(s)$ while PC-DIDIM succeeds in converging with, however, high relative errors.

We can explain the result as follows. One has $(\mathbf{q}_s, \dot{\mathbf{q}}_s, \ddot{\mathbf{q}}_s) \neq (\mathbf{q}, \dot{\mathbf{q}}, \ddot{\mathbf{q}})$ yielding $\mathbf{Z} \neq \mathbf{X}_{nf}$ at the last iteration of IDIM-IV and DIDIM. Besides, this gives $\hat{\boldsymbol{\Pi}} \neq \mathbf{I}_{n_b}$. However, $\mathbf{Z}$ being constructed with simulated data only, the IDM being assumed error-free, $\mathbf{Z}$ is not correlated with $\boldsymbol{\varepsilon}$. Then $E\left(\mathbf{Z}^T\boldsymbol{\varepsilon}\right) = \mathbf{0}$ holds.

We have $\hat{\boldsymbol{\beta}}_{IV} = \boldsymbol{\beta} + \left(\mathbf{Z}^T\mathbf{X}\right)^{-1}\mathbf{Z}^T\boldsymbol{\varepsilon}$, yielding $\text{plim}_{r\to\infty}\left(\hat{\boldsymbol{\beta}}_{IV}\right) = \boldsymbol{\beta} + \text{plim}_{r\to\infty}\left(\frac{1}{r}\mathbf{Z}^T\mathbf{X}\right)^{-1}\text{plim}_{r\to\infty}\left(\frac{1}{r}\mathbf{Z}^T\boldsymbol{\varepsilon}\right) = \boldsymbol{\beta}$.

Concerning the DIDIM estimates, one has $\hat{\boldsymbol{\beta}}_{DIDIM} = \left(\mathbf{Z}^T\mathbf{Z}\right)^{-1}\left(\mathbf{Z}^T\mathbf{X}\right)\boldsymbol{\beta} + \left(\mathbf{Z}^T\mathbf{Z}\right)^{-1}\mathbf{Z}^T\boldsymbol{\varepsilon}$. With $\mathbf{X} = \mathbf{Z}\hat{\boldsymbol{\Pi}} + \mathbf{V}$, it yields $E\left(\mathbf{Z}^T\mathbf{X}\right) = E\left(\mathbf{Z}^T\mathbf{Z}\hat{\boldsymbol{\Pi}}\right)$. This gives $\text{plim}_{r\to\infty}\left(\mathbf{Z}^T\mathbf{X}/r\right) = \text{plim}_{r\to\infty}\left(\mathbf{Z}^T\mathbf{Z}/r\right)\text{plim}_{r\to\infty}\hat{\boldsymbol{\Pi}} = \text{plim}_{r\to\infty}\left(\mathbf{Z}^T\mathbf{Z}/r\right)\boldsymbol{\Pi}$. Then this inserted into $\hat{\boldsymbol{\beta}}_{DIDIM}$ and with $E\left(\mathbf{Z}^T\boldsymbol{\varepsilon}\right) = \mathbf{0}$, we get $\text{plim}_{r\to\infty}\left(\hat{\boldsymbol{\beta}}_{DIDIM}\right) = \boldsymbol{\Pi}\boldsymbol{\beta} + \text{plim}_{r\to\infty}\left(\frac{1}{r}\mathbf{Z}^T\mathbf{Z}\right)^{-1}\text{plim}_{r\to\infty}\left(\frac{1}{r}\mathbf{Z}^T\mathbf{Z}\right) = \boldsymbol{\Pi}\boldsymbol{\beta}$.

By extension, we obtain the same conclusion with the PC-IDIM-IV and PC-DIDIM methods by inspection of (30). So, if errors are located in $C_j(s)$ only, the IDIM-IV estimates remain consistent, whereas the DIDIM estimates do not.

Interestingly, if $\hat{\boldsymbol{\beta}}_{DIDIM}$ is replaced by $\hat{\boldsymbol{\Pi}}^{-1}\hat{\boldsymbol{\beta}}_{DIDIM}$, then both DIDIM and PC-DIDIM converge and provide the same estimates as those of IDIM-IV and PC-IDIM-IV, respectively.

Compared with the relative errors given in Tables I and II, those of Tables V and VI are slightly greater; the cross-validation with the first joint and the first trajectory we have plotted in Fig. 4 confirms that. It comes out that the IDIM-IV and PC-IDIM-IV estimates are no longer optimal since $\mathbf{Z} \neq \mathbf{X}_{nf}$, and this is consistent with the theory developed in Section III-G.

F. Fifth scenario: error in the IDM

To conclude this study, we propose to run the IDIM-IV, PC-IDIM-IV, DIDIM, and PC-DIDIM methods with the

TABLE V
RELATIVE ERRORS OBTAINED WITH DIRECT VALIDATIONS - ERROR IN $C_j(s)$

Joint j	IDIM-IV	PC-IDIM-IV	PC-DIDIM
1	6.1%	5.9%	32.9%
2	6.3%	5.8%	33.5%
3	5.9%	5.5%	31.9%
4	6.4%	6.2%	32.7%
5	7.9%	7.6%	34.4%
6	8.1%	7.9%	35.0%

TABLE VI
RELATIVE ERRORS OBTAINED WITH CROSS-VALIDATION - ERROR IN $C_j(s)$

Traj.	IDIM-IV	PC-IDIM-IV	PC-DIDIM
1	7.1%	6.8%	45.7%
2	7.7%	7.2%	46.0%
3	8.1%	7.5%	45.1%

standard linear friction model (2) while inserting the low-velocity trajectories exhibiting a Stribeck effect of [52]. The IDM is, therefore, misspecified. All the methods have the same convergence performances as those obtained with the first scenario. Regarding the relative errors, they increase to 12 % because of the misspecified friction model. However, the estimates of the inertial parameters do not vary. We can explain this result as follows.

The IDM is *underspecified* because some variables are omitted in (8), see [40] chapter 3. We rewrite (8) as follows, see [37], [40],

$$\mathbf{y} = \mathbf{X}_{IN}\boldsymbol{\beta}_{IN} + \mathbf{X}_{OM}\boldsymbol{\beta}_{OM} + \boldsymbol{\varepsilon}_{clpt}\,, \tag{48}$$

where $\mathbf{X}_{IN} \in \mathbb{R}^{(r\times n_{in})}$ (resp. $\mathbf{X}_{OM} \in \mathbb{R}^{(r\times n_{om})}$) is the included (resp. omitted) observation matrix corresponding to $\boldsymbol{\beta}_{IN} \in \mathbb{R}^{n_{in}}$ (resp. $\boldsymbol{\beta}_{OM} \in \mathbb{R}^{n_{om}}$), the vector of included (resp. omitted) parameters; $\boldsymbol{\varepsilon}_{clpt} \in \mathbb{R}^r$ is the vector of errors corresponding to the *complete* regression. We assume that $\mathbf{X}_{OM}$ is orthogonal to the columns of $\mathbf{X}_{IN}$ yielding $\mathbf{X}_{OM}^T\mathbf{X}_{IN} = \mathbf{0}$, and so $E\left(\mathbf{X}_{OM}^T\mathbf{X}_{IN}\right) = \mathbf{0}$.

Let us assume that the effects encompassed by $\mathbf{X}_{OM}\boldsymbol{\beta}_{OM}$ occur at low frequencies, such as friction. Then, $C_j(s)$ rejects them like any low-frequency disturbance, and $(\mathbf{q}_s, \dot{\mathbf{q}}_s, \ddot{\mathbf{q}}_s) \approx (\mathbf{q}, \dot{\mathbf{q}}, \ddot{\mathbf{q}})$ still holds, see [10], [12]. It follows that both the IDIM-IV and DIDIM estimates of $\boldsymbol{\beta}_{IN}$ are consistent since we have $E\left(\mathbf{Z}_{IN}^T\boldsymbol{\varepsilon}_{clpt}\right) = \mathbf{0}$. This result is still valid even in the nonlinear case, i.e., when $\mathbf{X}_{OM}\boldsymbol{\beta}_{OM}$ is substituted by $\boldsymbol{f}_{OM}(\boldsymbol{\beta}_{OM}) \in \mathbb{R}^r$. Indeed, assuming that $\boldsymbol{f}_{OM}(\boldsymbol{\beta}_{OM})$ occur at low frequencies, $C_j(s)$ rejects them, giving $(\mathbf{q}_s, \dot{\mathbf{q}}_s, \ddot{\mathbf{q}}_s) \approx (\mathbf{q}, \dot{\mathbf{q}}, \ddot{\mathbf{q}})$ and so $E\left(\mathbf{Z}_{IN}^T\boldsymbol{\varepsilon}_{cplt}\right) = \mathbf{0}$.

It comes out that we obtained the same result with the PC-IDIM-IV and PC-DIDIM methods. Indeed, under these circumstances, we get $(\mathbf{q}_s, \dot{\mathbf{q}}_s, \ddot{\mathbf{q}}_s) \approx (\mathbf{q}, \dot{\mathbf{q}}, \ddot{\mathbf{q}})$ giving $E\left(\mathbf{Z}_{IN}^T\boldsymbol{\varepsilon}_{clpt}\right) = \mathbf{0}$ and $\hat{\boldsymbol{\mu}} \to \mathbf{0}$ since the constraints are satisfied. These are the conditions to get consistent PC-IDIM-IV and PC-DIDIM estimates. It is a unique case where we can choose PC-IDIM-IV and PC-DIDIM indifferently.

This result is crucial because it explains why separable approaches are suitable for nonlinear friction identification, provided that friction is not load-dependent. In such a case, separable methods are unsuitable since friction can be considered dynamic, and we must run more sophisticated identification methods. This explains the good results presented in [7], [36], [53].

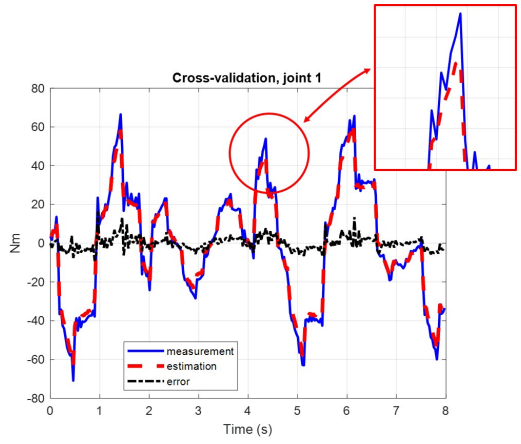

Fig. 4. Cross-validation, first joint, and first trajectory with error in $C_j(s)$.

V. CONCLUSION

In this paper, we have presented a constrained instrumental variable method for industrial robot identification, called PC-IDIM-IV, Physically Consistent Inverse Dynamic Identification Model with Instrumental Variable, and validated it on the 6-DOF industrial robot TX40.

This method validates the direct and inverse dynamic models and consists of two nested iterative algorithms: the outer one which is the usual IV method, and the inner one which solves the physical constraints with the Gauss-Newton algorithm. In the theoretical analysis, we analyzed the consistency of PC-IDIM-IV estimates and the effect of constraints. The experimental results showed that PC-IDIM-IV is consistent when the inverse dynamical model is error-free, and/or when there is an error in the controller, and is less sensitive to modeling errors than other approaches, provided the problem remains feasible. Besides, they showed that the constraints we have proposed are not overly restrictive and PC-IDIM-IV is not time-consuming: 60 dynamic parameters are identified in less than one minute. This result offers some good perspectives for batching online identification.

Future works concern batching online applications of the PC-IDIM-IV to identify the TX40 and KUKA LBR iiwa 14 R820 robots.

VI. APPENDICES

A. Comments on the data filtering

The works published in Automatic Control mostly use (7) by assuming that $\varepsilon_{m_j} = H_j(z^{-1})e_j$, where ε_{m_j} is the joint j error, $H_j(z^{-1})$ is a stable discrete filter with z^{-1} as the shift operator, and e_j a white noise whose variance is σ_j^2. Then, we identify $H_j(z^{-1})$ with standard procedures as described in [11], [13], [28] to get $\hat{H}_j(z^{-1})$.

Let $\mathbf{X}_{m_j}$, $\mathbf{Z}_{m_j}$ and $\mathbf{y}_{m_j}$ resulting from the sampling of $\mathbf{IDM}_j(\hat{\mathbf{q}}, \hat{\dot{\mathbf{q}}}, \hat{\ddot{\mathbf{q}}})$, $\mathbf{IDM}_j(\mathbf{q}_S, \dot{\mathbf{q}}_S, \ddot{\mathbf{q}}_S)$, and τ_j, respectively. With $\mathbf{X}^f$, $\mathbf{Z}^f$, and $\mathbf{y}^f$ resulting from the vertical stacking of the $\mathbf{X}_j^f$'s, $\mathbf{Z}_j^f$'s and $\mathbf{y}_j^f$'s, respectively, with $\mathbf{X}_j^f = \hat{H}_j^{-1}(z^{-1})\mathbf{X}_{m_j}$, $\mathbf{Z}_j^f = \hat{H}_j^{-1}(z^{-1})\mathbf{Z}_{m_j}$, and $\mathbf{y}_j^f = \hat{H}_j^{-1}(z^{-1})\mathbf{y}_{m_j}$, we substitute $\mathbf{X}$, $\mathbf{Z}$ and $\mathbf{y}$ by $\mathbf{X}^f$, $\mathbf{Z}^f$ and $\mathbf{y}^f$, respectively, in (28). However, [54] shows that this process does not improve the parallel decimation process. Consequently, we suggest running the filtering procedure described in [43] and recalled in Section II-C.

B. Proof of $rank\left(\hat{\mathbf{\Pi}}\right) = n_b$ implies $rank\left(\mathbf{\Pi}\right) = n_b$

We have $\hat{\mathbf{\Pi}} = \left(\mathbf{Z}^T\mathbf{Z}\right)^{-1}\mathbf{Z}^T\mathbf{X}$, since $rank(\mathbf{Z}) = n_b$, one has $rank\left(\mathbf{Z}^T\mathbf{Z}\right) = n_b$ and so $\mathbf{Z}^T\mathbf{Z} \succ \mathbf{0}$. Because $rank\left(\mathbf{Z}^T\mathbf{X}\right) = n_b$ by assumption, $rank\left(\hat{\mathbf{\Pi}}\right) = n_b$ follows. Assuming $\text{plim}_{r\to\infty}\left(\frac{1}{r}\mathbf{Z}^T\mathbf{Z}\right)$ converges to a deterministic and finite matrix with rank n_b (likewise for $\text{plim}_{r\to\infty}\left(\frac{1}{r}\mathbf{Z}^T\mathbf{X}\right)$), and since $E\left(\mathbf{Z}^T\mathbf{V}\right) = \mathbf{0}$, it follows $\text{plim}_{r\to\infty}\left(\hat{\mathbf{\Pi}}\right) = \text{plim}_{r\to\infty}\left(\frac{1}{r}\mathbf{Z}^T\mathbf{Z}\right)^{-1}\text{plim}_{r\to\infty}\left(\frac{1}{r}\mathbf{Z}^T\mathbf{X}\right) = \mathbf{\Pi}$, with $rank\left(\mathbf{\Pi}\right) = n_b$.

Note that the existence of $\text{plim}_{r\to\infty}\left(\hat{\mathbf{\Pi}}\right)$ implies the existence of $\text{plim}_{r\to\infty}\left(\frac{1}{r}\mathbf{Q}_{ZX}\right) = \text{plim}_{r\to\infty}\left(\frac{1}{r}\hat{\mathbf{X}}^T\mathbf{X}\right)$.

C. Proof of the 2SLS estimates reduce to the IV estimates when $n_z = n_b$

We have $\hat{\boldsymbol{\beta}}_{2SLS} = \left(\hat{\mathbf{X}}^T\mathbf{X}\right)^{-1}\hat{\mathbf{X}}^T\mathbf{y}$, $\hat{\boldsymbol{\beta}}_{2SLS} = \left(\mathbf{X}^T\mathbf{Z}\left(\mathbf{Z}^T\mathbf{Z}\right)^{-1}\mathbf{Z}^T\mathbf{X}\right)^{-1}\left(\mathbf{X}^T\mathbf{Z}\left(\mathbf{Z}^T\mathbf{Z}\right)^{-1}\mathbf{Z}^T\right)\mathbf{y}$, $\hat{\boldsymbol{\beta}}_{2SLS} = \left(\mathbf{Z}^T\mathbf{X}\right)^{-1}\mathbf{Z}^T\mathbf{Z}\left(\mathbf{X}^T\mathbf{Z}^T\right)^{-1}\mathbf{X}^T\mathbf{Z}\left(\mathbf{Z}^T\mathbf{Z}\right)^{-1}\mathbf{Z}^T\mathbf{y}$, $\hat{\boldsymbol{\beta}}_{2SLS} = \left(\mathbf{Z}^T\mathbf{X}\right)^{-1}\mathbf{Z}^T\mathbf{Z}\left(\mathbf{Z}^T\mathbf{Z}\right)^{-1}\mathbf{Z}^T\mathbf{y}$, $\hat{\boldsymbol{\beta}}_{2SLS} = \left(\mathbf{Z}^T\mathbf{X}\right)^{-1}\mathbf{Z}^T\mathbf{y}$, $\hat{\boldsymbol{\beta}}_{2SLS} = \hat{\boldsymbol{\beta}}_{IV}$, because $rank\left(\mathbf{Z}^T\mathbf{X}\right) = n_b$ by assumption.

D. Justification of the relation between the unconstrained and constrained IV estimates

First, we can write

$$\mathbf{y} = \mathbf{X}_C\boldsymbol{\beta}^C + \mathbf{X}_U\boldsymbol{\beta}^U + \boldsymbol{\varepsilon}\,, \tag{49}$$

then with $\boldsymbol{\beta}^C = \mathbf{d}$, one gets

$$\hat{\boldsymbol{\beta}}_{CIV}^U = \left(\mathbf{Z}_U^T\mathbf{X}_U\right)^{-1}\mathbf{Z}_U^T\left(\mathbf{y} - \mathbf{X}_C\mathbf{d}\right)\,. \tag{50}$$

With the unconstrained IV estimates, one has

$$\mathbf{y} = \mathbf{X}_C\hat{\boldsymbol{\beta}}_{IV}^C + \mathbf{X}_U\hat{\boldsymbol{\beta}}_{IV}^U + \hat{\boldsymbol{\varepsilon}}_{IV}\,, \tag{51}$$

where $\hat{\boldsymbol{\varepsilon}}_{IV} \in \mathbb{R}^r$ is the IV residuals. Since $\hat{\boldsymbol{\beta}}_{IV}^C$ and $\hat{\boldsymbol{\beta}}_{IV}^U$ are consistent estimates of $\boldsymbol{\beta}^C$ and $\boldsymbol{\beta}^U$, $\hat{\boldsymbol{\varepsilon}}_{IV}$ is a consistent estimate of $\boldsymbol{\varepsilon}$, [55]. Besides, $\hat{\boldsymbol{\varepsilon}}_{IV}$ is orthogonal to the columns of $\mathbf{Z}_U$ by geometrical construction, [37], chapter 1. One finally obtains

$$\hat{\boldsymbol{\beta}}_{CIV}^U = \hat{\boldsymbol{\beta}}_{IV}^U + \left(\mathbf{Z}_U^T\mathbf{X}_U\right)^{-1}\mathbf{Z}_U^T\mathbf{X}_C\left(\hat{\boldsymbol{\beta}}_{IV}^C - \mathbf{d}\right)\,. \tag{52}$$

REFERENCES

[1] Q. Leboutet, J. Roux, A. Janot, J. R. Guadarrama-Olvera, and G. Cheng, "Inertial parameter identification in robotics: A survey," *Applied Sciences*, vol. 11, no. 9, p. 4303, 2021.

[2] K. Ayusawa, G. Venture, and Y. Nakamura, "Identifiability and identification of inertial parameters using the underactuated base-link dynamics for legged multibody systems," *Int. J. of Robotics Research*, vol. 33, no. 3, pp. 446–468, 2014.

[3] J. Jovic, A. Escande, K. Ayusawa, E. Yoshida, A. Kheddar, and G. Venture, "Humanoid and human inertia parameter identification using hierarchical optimization," *IEEE Transactions on Robotics*, vol. 32, no. 3, pp. 726–735, June 2016.

[4] E. Villagrossi, L. Simoni, M. Beschi, N. Pedrocchi, A. Marini, L. M. Tosatti, and A. Visioli, "A virtual force sensor for interaction tasks with conventional industrial robots," *Mechatronics*, vol. 50, pp. 78 – 86, 2018. [Online]. Available: http://www.sciencedirect.com/science/article/pii/S0957415818300163

[5] C. Semini, V. Barasuol, T. Boaventura, M. Frigerio, M. Focchi, D. G. Caldwell, and J. Buchli, "Towards versatile legged robots through active impedance control," *The International Journal of Robotics Research*, vol. 34, no. 7, pp. 1003–1020, 2015. [Online]. Available: http://ijr.sagepub.com/content/34/7/1003.abstract

[6] P. M. Wensing, A. Wang, S. Seok, D. Otten, J. Lang, and S. Kim, "Proprioceptive actuator design in the MIT Cheetah: Impact mitigation and high-bandwidth physical interaction for dynamic legged robots," *IEEE Transactions on Robotics*, vol. 33, no. 3, pp. 509–522, 2017.

[7] Y. Han, J. Wu, C. Liu, and Z. Xiong, "An iterative approach for accurate dynamic model identification of industrial robots," *IEEE Transactions on Robotics*, vol. 36, no. 5, pp. 1577–1594, 2020.

[8] Y. Huang, J. Ke, X. Zhang, and J. Ota, "Dynamic parameter identification of serial robots using a hybrid approach," *IEEE Transactions on Robotics*, pp. 1–15, 2022.

[9] D. Jung, H. Do, T. Choi, J. Park, and J. Cheong, "Robust parameter estimation of robot manipulators using torque separation technique," *IEEE Access*, vol. 9, pp. 150 443–150 458, 2021.

[10] M. Gautier, A. Janot, and P.-O. Vandanjon, "A new closed-loop output error method for parameter identification of robot dynamics," *IEEE Transactions on Control Systems Technology*, vol. 21, no. 2, pp. 428–444, 2012.

[11] P. C. Young, *Recursive estimation and time-series analysis: An introduction for the student and practitioner*. Springer Science & Business Media, 2011.

[12] A. Janot, P.-O. Vandanjon, and M. Gautier, "A generic instrumental variable approach for industrial robot identification," *IEEE Transactions on Control Systems Technology*, vol. 22, no. 1, pp. 132–145, 2014.

[13] L. Ljung, *System Identification: Theory for the User (2nd Edition)*. Prentice Hall, 1999.

[14] C. D. Sousa and R. Cortesao, "Physical feasibility of robot base inertial parameter identification: A linear matrix inequality approach," *The International Journal of Robotics Research*, vol. 33, no. 6, pp. 931–944, 2014.

[15] P. M. Wensing, S. Kim, and J.-J. E. Slotine, "Linear matrix inequalities for physically consistent inertial parameter identification: A statistical perspective on the mass distribution," *IEEE Robotics and Automation Letters*, vol. 3, no. 1, pp. 60–67, 2018.

[16] Y. R. Stürz, L. M. Affolter, and R. S. Smith, "Parameter identification of the kuka lbr iiwa robot including constraints on physical feasibility," *IFAC-PapersOnLine*, vol. 50, no. 1, pp. 6863–6868, 2017.

[17] C. D. Sousa and R. Cortesão, "Inertia tensor properties in robot dynamics identification: A linear matrix inequality approach," *IEEE/ASME Transactions on Mechatronics*, vol. 24, no. 1, pp. 406–411, Feb 2019.

[18] C. Gaz, M. Cognetti, A. Oliva, P. R. Giordano, and A. De Luca, "Dynamic identification of the franka emika panda robot with retrieval of feasible parameters using penalty-based optimization," *IEEE Robotics and Automation Letters*, vol. 4, no. 4, pp. 4147–4154, 2019.

[19] A. Janot and P. M. Wensing, "Sequential semidefinite optimization for physically and statistically consistent robot identification," *Control Engineering Practice*, vol. 107, p. 104699, 2021.

[20] F. Wolak, "An exact test for multiple inequality and equality constraints in the linear regression model," *Journal of the American Statistical Association*, vol. 82, no. 399, pp. 782–793, 1987.

[21] ——, "Testing inequality constraints in linear econometric models," *Journal of Econometrics*, vol. 41, pp. 205–235, 1989.

[22] ——, "Local and global testing of linear and nonlinear inequality constraints in nonlinear econometric models," *Econometric theory*, vol. 5, pp. 1–35, 1989.

[23] G. W. Imbens and J. D. Angrist, "Identification and estimation of local average treatment effects," *Econometrica*, vol. 62, no. 2, pp. 467–475, 1994.

[24] C. Gourieroux and A. Monfort, *Statistics and Econometric Models Vol.1*. Cambridge University Press, 1995.

[25] ——, *Statistics and Econometric Models Vol.2*. Cambridge University Press, 1995.

[26] D. Chetverikov, A. Santos, and A. M. Shaikh, "The econometrics of shape restrictions," *Annual Review of Economics*, vol. 10, pp. 31–63, 2018.

[27] Y.-W. Hsieh, X. Shi, and M. Shum, "Inference on estimators defined by mathematical programming," *Journal of Econometrics*, vol. 226, p. 248–268, 2022.

[28] P. C. Young, "Refined instrumental variable estimation: Maximum likelihood optimization of a unified box–jenkins model," *Automatica*, vol. 52, pp. 35–46, 2015. [Online]. Available: https://www.sciencedirect.com/science/article/pii/S0005109814005147

[29] W. Khalil and E. Dombre, *Modeling identification and control of robots*. CRC Press, 2002.

[30] M. Gautier and W. Khalil, "Direct calculation of minimum set of inertial parameters of serial robots," *IEEE Transactions on robotics and Automation*, vol. 6, no. 3, pp. 368–373, 1990.

[31] É. Walter and L. Pronzato, *Identification de modèles paramétriques à partir de données expérimentales*. Masson, 1994.

[32] S. Boyd and L. Vandenberghe, *Convex optimization*. Cambridge University Press, 2009.

[33] M. Grant and S. Boyd, "CVX: Matlab software for disciplined convex programming, version 2.1," http://cvxr.com/cvx, Mar. 2014.

[34] F. Ardiani, A. Janot, and B. Mourad, "Industrial robot parameter identification using a constrained instrumental variable method," in *Proceedings 2022 IEEE/RSJ International Conference on Intelligent Robots and Systems*, vol. XX. IEEE, 2022, pp. 1–6.

[35] B. Siciliano, L. Sciavicco, L. Villani, and G. Oriolo, *Robotics: modelling, planning and control*. Springer Science & Business Media, 2010.

[36] M. Indri and S. Trapani, "Framework for static and dynamic friction identification for industrial manipulators," *IEEE/ASME Transactions on Mechatronics*, vol. 25, no. 3, pp. 1589–1599, 2020.

[37] R. Davidson and J. MacKinnon, *Estimation and Inference in Econometrics*. Oxford University Press, 1993.

[38] ——, *Econometric theory and methods*. Oxford University Press, 2004.

[39] H. White, *Asymptotic Theory for Econometricians*. Elsevier, 1984.

[40] J. M. Wooldridge, *Introductory Econometrics: A Modern Approach*. South-Western College Publishing, 2012.

[41] T. Soderstrom and P. Stoica, *Instrumental Variable Methods for System Identification*. Springer Verlag Berlin, 1983.

[42] ——, *System Identification*. Prentice-Hall International, Hemel Hempstead, U.K, 1989.

[43] M. Gautier and G. Venture, "Identification of standard dynamic parameters of robots with positive definite inertia matrix," in *2013 IEEE/RSJ International Conference on Intelligent Robots and Systems*. IEEE, 2013, pp. 5815–5820.

[44] T. Xu, J. Fan, Y. Chen, X. Ng, M. H. Ang, Q. Fang, Y. Zhu, and J. Zhao, "Dynamic identification of the kuka lbr iiwa robot with retrieval of physical parameters using global optimization," *IEEE Access*, vol. 8, pp. 108 018–108 031, 2020.

[45] J. H. Stock, J. H. Wright, and M. Yogo, "A survey of weak instruments and weak identification in generalized method of moments," *Journal of Business & Economic Statistics*, vol. 20, no. 4, pp. 518–529, 2002.

[46] D. Staiger and J. H. Stock, "Instrumental variables regression with weak instruments," *Econometrica*, vol. 65, no. 3, pp. 557–586, 1997.

[47] S. Boyd and L. Vandenberghe, *Introduction to Applied Linear Algebra*. Cambridge University Press, 2018.

[48] L. Vandenberghe, "The cvxopt linear and quadratic cone program solvers," *Documentation*, March 2010. [Online]. Available: http://cvxopt.org/documentation/coneprog.pdf

[49] A. Janot, P.-O. Vandanjon, and M. Gautier, "A revised durbin-wu-hausman test for industrial robot identification," *Control Engineering Practice*, vol. 48, pp. 52–62, 2016.

[50] M. Gautier and W. Khalil, "Exciting trajectories for the identification of base inertial parameters of robots," *The International journal of robotics research*, vol. 11, no. 4, pp. 362–375, 1992.

[51] J. Swevers, C. Ganseman, D. B. Tukel, J. De Schutter, and H. Van Brussel, "Optimal robot excitation and identification," *IEEE transactions on robotics and automation*, vol. 13, no. 5, pp. 730–740, 1997.

[52] A. Janot, "A separable instrumental variable method for robot identification," in *2021 American Control Conference (ACC)*, 2021, pp. 4339–4344.

[53] S. M. Hashemi and H. Werner, "Parameter identification of a robot arm using separable least squares technique," in *2009 European Control Conference (ECC)*, Aug 2009, pp. 2199–2204.

[54] M. Brunot and A. Janot, "A new recursive instrumental variables approach for robot identification," *IFAC-PapersOnLine*, vol. 51, pp. 132–137, 10 2018.

[55] H. White, "A heteroskedasticity-consistent covariance matrix estimator and a direct test for heteroskedasticity," *Econometrica*, vol. 48, no. 4, pp. 817–838, 1980.